EJTAS
ISSN 2786-7447
EUROPEAN JOURNAL OF THEORETICAL AND APPLIED SCIENCES
OPEN ACCESS
PEER REVIEWED

Impact of Different Groups on Properties of All Members of the Series of 1-X-Benzotriazole Derivatives (X= H, OH, NH_2, C_l and CH_3)

María E. Manzur
Cátedra de Química General, Instituto de Química Inorgánica, Facultad de Bioquímica. Química y Farmacia, Universidad Nacional de Tucumán, Tucumán, Argentina

Maximiliano A. Iramain
Cátedra de Química General, Instituto de Química Inorgánica, Facultad de Bioquímica. Química y Farmacia, Universidad Nacional de Tucumán, Tucumán, Argentina

Vahidreza Darugar
Department of Chemistry, Faculty of Science, Ferdowsi University of Mashhad, Mashhad, Iran

Mohammad Vakili
Department of Chemistry, Faculty of Science, Ferdowsi University of Mashhad, Mashhad, Iran

Silvia Antonia Brandán *
Cátedra de Química General, Instituto de Química Inorgánica, Facultad de Bioquímica. Química y Farmacia, Universidad Nacional de Tucumán, Tucumán, Argentina

Article Information

Suggested Citation:
Manzur, M.E., Iramain, M.A., Darugar, V., Vakili, M. & Brandán, S.A. (2023). Impact of different groups on properties of all members of the series of 1-X-benzotriazole derivatives (X= H, OH, NH_2, C_l and CH_3). *European Journal of Theoretical and Applied Sciences, 1*(3), 406-440.
DOI: 10.59324/ejtas.2023.1(3).42

*** Corresponding author:**
Silvia Antonia Brandán
e-mail:
silvia.brandan@fbqf.unt.edu.ar

Abstract:

Here, the impact of different groups on the geometrical parameters, dipole moments, atomic charges, stabilization and solvation energies, molecular electrostatic potentials, densities rings, positions IR and UV bands and NMR chemical shifts of all members of the series of 1X-benzotriazole derivatives (X= H, CH_3, Cl, NH_2 and OH) have been investigated by using hybrid B3LYP/6-311++G** calculations because, so far, correlations among their properties neither the vibrational analyses are reported yet. The polarity of N-X bonds, electronegativity, donor/acceptor characteristics of the different X groups were analysed for all members. The polarity of N1-X4 bonds have influence on dipole moments, volumes and on bond lengths of both rings while the chlorinated derivative has a higher reactivity due to its higher global electrophilicity index. NBO and AIM studies reveal the strong influence of Cl on densities of both rings of CBT and, on this derivative. Harmonic force fields evidence very good correlations between stretching force constants and assignments.

Keywords: *Benzotriazole derivatives; Molecular structure; Electronegativity; Force fields; DFT calculations.*

Introduction

In this investigation the series of 1-X-benzotriazole derivatives with X= H, CH_3, Cl, NH_2 and OH have been studied by using functional hybrid B3LYP/6-311++G** calculations in order to analyse how the characteristics of different groups have influence on their structures, properties, behaviours and reactivities. These types of studies are very important for the design of new and improved

drugs, taking into account that the uses and applications of these derivatives are very different between them. Thus, 1-Aminobenzotriazole (ABT) has been used from long time as an inhibitor of cytochrome P450 enzymes (Mugford et al., 1992; Emoto et al., 2003; Sun et al., 2011; Parrish et al., 2015; Watanabe et al., 2016; Shaik et al., Ortiz de Montellano, 2018) while 1-Hidroxybenzotriazole (HOBT) has multiple uses because it has explosive properties, is a reactive broadly used in organic chemistry as oxidant agent and, in addition, it can inhibit the copper corrosion, as was also reported for 1-Methylbenzotriazole (MBT) (Wehrstedt et al., 2005; Vemula et al., 2005; Hirai et al., 2006; Malow et al., 2007; Finšgar & Milošev, 2010; Kokalj et al., 2010; Chen et al., 2014; Asimakopoulos et al., 2013; Santiago et al., 2018; Shi et al., 2019; Pacheco-Juárez et al., 2019; Kotowska et al., 2021). Besides, these derivatives widely used in many applications undergoes transformations with the exposure to UV light and represent the fourth most abundant aquatic contaminants and, for these reasons, they are also very important from environmental point of view (Asimakopoulos et al., 2013; Santiago et al., 2018; Shi et al., 2019; Pacheco-Juárez et al., 2019; Kotowska et al., 2021). Recently, a study on a benzotriazole derivative bonded to a quinolone ring has evidenced a reactivity higher than antiviral chloroquine (Karrouchi et al., 2023). Hence, potential pharmacological applications as antiviral agent could be expected in some of these derivatives (Karrouchi et al., 2023). For all these backgrounds, the structural studies related to the benzotriazole moiety linked to the different groups are important to understand how the characteristics and nature of different H, OH, NH_2, Cl and CH_3 groups have influence and effect on the properties, activities, ^{1}H- and ^{13}C-NMR chemical shifts, positions of IR and UV-Vis bands of those derivatives. Here, the aims of this work are first the optimizations of 1-H-benzotriazole (HBT), 1-Methyl-benzotriazole (MBT), 1-Cl-benzotriazole (CBT), 1-Amino-benzotriazole (ABT) and 1-Hidroxy-benzotriazole (HOBT) species in gas phase and aqueous solution by using B3LYP/6-311++G** calculations (Becke, 1988; Lee et al., 1988). After that, the polarized continuum method (PCM) and solvation universal model, natural bond orbital (NBO) and atoms in molecules (AIM) calculations were performed to calculate solvation energies, atomic charges, stabilization energies and topological properties. In addition, the frontier orbitals studies are very important to know differences in their reactivities and behaviours in both environments while to know the effects of groups on the positions and intensities of IR bands the determination of harmonic force fields and the scaled force constants are necessaries.

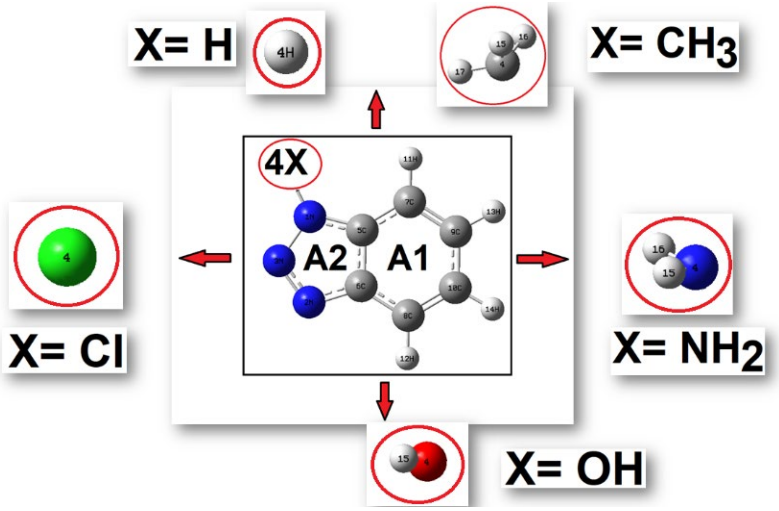

Figure 1. Structures of All Members of the Series of 1X-Benzotriazole Derivatives (X= H, CH_3, C_l, NH_2 and OH) with Definitions of Rings and Atoms Labelling

Table 1. Molecular Formula and Weight of all Members of Series of 1-X-Benzotriazole Derivatives (X= H, CH_3, C_l, NH_2, OH) Showing the Electronegativity, Character and Polarity of N-X Bonds of Involved Groups

Derivative	Molecular Formula	Molecular Weight	Group	Electronegativity	Character	Polarity N1-X4
HBT	$C_6H_5N_3$	119.12	H	2.10	Neutral	0.9
MBT	$C_7H_7N_3$	133.15	CH_3	2.55	Activating weak	0.5
CBT	$C_6H_4ClN_3$	153.57	Cl	3.00	Deactivating weak	0
ABT	$C_6H_6N_4$	134.14	NH_2	3.12	Activating strong	0
HOBT	$C_6H_5N_3O$	135.12	OH	3.55	Activating strong	0.5

Note: 1-H-benzotriazole (HBT), 1-Methyl-benzotriazole (MBT), 1-Cl-benzotriazole (CBT), 1-Amino-benzotriazole (ABT) and 1-Hidroxy-benzotriazole (HOBT)

Here, the effect of electronegativities of groups, polarities of bonds, hydrophobic/hydrophilic nature, activating/deactivating and acceptor/donor character of different groups on the predicted properties of all members of the series have been carefully evaluated. The series of studied compounds with the atoms labelling and identification of both rings can be seen in Figure 1 while in Table 1 are summarized the molecular formula and weight of series of 1-X-Benzotriazole derivatives showing the electronegativity of group (X), character and polarity of N-X bonds of all derivatives. Electronegativity values of groups were taken from those reported by Gupta (2016). The results presented in interesting figures and graphics show modifications in the properties, reactivities and behaviours of those derivatives with the different media as function of electronegativity of X, polarity of bond N-X and hydrophobic/hydrophilic nature or activating/deactivating character of X (Darugar et al., 2023).

Computational Approaches

All calculations of series of benzotriazole derivatives in gas phase and aqueous solution were performed with the hybrid B3LYP/6-311++G** and IEF-PCM methods, the universal solvation method (SMD) and Gaussian 09 program (Frisch et al., 2009; Miertus et al., 1981; Tomasi & Persico, 1994; Marenich et al., 2009). The permittivity of water was taken as 78.36 (Frisch et al., 2009). The modelled of 1-H-benzotriazole (HBT), 1-Methyl-benzotriazole (MBT), 1-Cl-benzotriazole (CBT), 1-Amino-benzotriazole (ABT) and 1-Hidroxy-benzotriazole (HOBT) species was carried out with the *GaussView* program (Nielsen & Holder, 2008). NBO 5.1 and AIM 2000 programs were used to compute charges, ring's density, stabilization's energy while the molecular electrostatic potentials were calculated with Merz-Kollman (MK) charges (Glendening et al., 1996; Bader, 1990; Biegler-Köning et al., 2001; Besler et al., 1990). Gap values together with chemical potential, electronegativity, global hardness, global softness and global electrophilicity index descriptors were predicted by using the frontier orbitals and typical equations (Lee et al., 1988; Parr & Pearson, 1983). Changes in the volumes were evaluated with the Moldraw program (Ugliengo, 1998). The ^{1}H and ^{13}C NMR spectra of all species in aqueous solution were predicted with the GIAO method while the electronic spectra in aqueous solution with the Gaussian 09 program (Frisch et al., 2009; Ditchfield, 1974). Complete vibrational assignments for all members of the series were performed with the harmonic force fields using the SQMFF methodology and the Molvib program (Pulay et al., 1983; Rauhut & Pulay, 1995; Sundius, 2002).

Results and Discussion

Optimizations of All Members of the Series

Figure 1 shows the benzotriazole ring that is the common part in all derivatives while the X4

atom change in each derivative, thus, X4 is H in HBT; CH_3 in MBT; Cl in CBT; NH_2 in ABT and OH in HOBT. Figure S1 shows the structures of all derivatives with the atoms labelling. The results of optimizations of HBT, MBT, CBT, ABT and HOBT in the different environments are shown in Table 2.

Table 2. Calculated total (E) and Corrected by ZPVE Energies (EZPVE), Dipole Moments (μ) and Volumes (V) for All Members of Series of 1-X-Benzotriazole Derivatives (X= H, CH_3, Cl, NH_2, OH) in Gas Phase and Aqueous Solution by Using the B3LYP/6-311++G(d,p) Method. Differences of Energy (ΔG) and Volume Values are Also Included

B3LYP/6-311++G** Method							
1-H-BENZOTRIAZOLE (HBT)							
Medium	E (Hartrees)	E_{ZPVE}	μ(D)	V(Å^3)	ΔV(Å^3)	ΔG(kJ/Mol)	ΔG_{ZPVE}(kJ/Mol)
Gas	-395.9709	-395.8655	4.19	108.5	-0.9	-45.11	-44.33
Water	-395.9881	-395.8824	6.20	107.6			
1-METHYL-BENZOTRIAZOLE (MBT)							
Medium	E (Hartrees)	E_{ZPVE}	μ(D)	V(Å^3)		ΔG(kJ/Mol)	ΔG_{ZPVE}(kJ/Mol)
Gas	-435.2944	-435.1613	4.29	143.2	-0.4	-38.03	-36.98
Water	-435.3089	-435.1754	6.55	142.8			
1-CL-BENZOTRIAZOLE (CBT)							
Medium	E (Hartrees)	E_{ZPVE}	μ(D)	V(Å^3)		ΔG(kJ/Mol)	ΔG_{ZPVE}(kJ/Mol)
Gas	-855.5417	-855.4468	3.98	140.4	-1.0	-27.70	-25.18
Water	-855.5515	-855.4564	5.87	139.4			
1-AMINO-BENZOTRIAZOLE (ABT)							
Medium	E (Hartrees)	E_{ZPVE}	μ(D)	V(Å^3)		ΔG(kJ/Mol)	ΔG_{ZPVE}(kJ/Mol)
Gas	-451.3120	-451.1898	3.16	137.2	0.4	-41.97	-42.23
Water	-451.3280	-451.2059	4.59	137.6			
1-HIDROXY-BENZOTRIAZOLE (HOBT)							
Medium	E (Hartrees)	E_{ZPVE}	μ(D)	V(Å^3)		ΔG(kJ/Mol)	ΔG_{ZPVE}(kJ/Mol)
Gas	-471.1545	-471.0459	3.75	133.5	0.1	-46.16	-45.90
Water	-471.1721	-471.0634	6.33	133.6			

Thus, the table shows calculated total and corrected by ZPVE energies, dipole moments, differences of energy (ΔG), and, V and ΔV volume for the series of 1-X-Benzotriazole derivatives in both media by using the B3LYP/6-311++G(d,p) method. (ΔG) values are calculated from differences of E in solution –E gas phase while ΔG_{ZPVE} is the differences between E_{ZPVE} in solution –E_{ZPVE} gas phase. Note that ΔG_{ZPVE} have higher values than the corresponding to ΔG. The E values are corrected by zero-point vibrational energies (ZPVE) because the molecules present movements even in the zero K. Dipole moments (μ) and volumes of all the members of the series as a function of the electronegativities of X4 can be observed in Figure 2 while in Figure 3 are shown the orientations, magnitudes and directions of μ vectors of all members of the series.

Regarding Figure 2a, we observed that the μ values of all members of the series in gas phase do not present a defined trend because they do not increase with electronegativity, however in solution, μ of the HBT, MBT and HOBT derivatives increase when the electronegativity increases, with the exception of the CBT and ABT derivatives which decrease as the electronegativity increases. Such differences could be explained with the polarity of the N-Cl and N-N bonds, since both present null polarity.

These values are calculated from the differences in the electronegativity values, thus, the N-Cl bond in CBT has a polarity value of 3.0 (N)-3.0 (Cl) = 0 while the value in ABT is of 3.0 (N)- 3.0 (N)= 0. Besides, the μ values for CBT in both environments are different from ABT because the Cl is a deactivating agent which implies that it attracts electrons by inductive effect and, as a consequence causes bond elongation while the amino groups is strong activating and, for this reason, as we see later, the N1-N4 distance (1.388 Å) is lower than the N1-Cl4 (1.699 Å) one. Evaluating the volumes of all derivatives from Figure 2b, we observed that they present the same behaviours in both media and only the volumes of first two members of series increase with the electronegativity while V of remaining members decrease conform increase the electronegativity. Here, evidently the hydrophilic and/or strong activating character of X has influence on V because the NH_2 and OH groups are donor´s H bonds and they are hydrated in solution, hence, they present the lower V values together with HBT while the Cl of higher size has possibly low hydration level.

When V for all derivatives are graphed as function of molecular weights (MW) from Figure S2 we observed that despite of the proximities of MWs of MBT, ABT and HOBT derivatives the Vs are different among them. Hence, CBT with higher MW presents a lower V than MBT. Thus, the differences in volumes cannot be explained with the MWs.

If now Figure 3 is analysed it is observed that the μ vectors of all the members of the series change of magnitudes in solution but the vectors of CBT, ABT and HOBT undergoes changes in direction and orientation being more evident in CBT and HOBT. Probably, the higher hydrations of the donors of H bonds groups and the different V values explain their behaviours and changes in solution because the CBT derivative undergoes V contraction while expansions of V are observed in ABT and HOBT. These studies show that polarity of the N1-X4 bonds and the hydrophilic and/or strong donor character of X have influence on μ and volumes of all benzotriazole derivative while the MWs don't explain the differences observed.

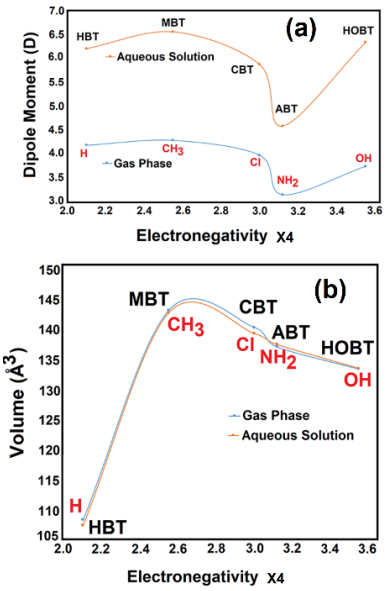

Figure 2. Variations of Dipole Moment (upper) and Volumes (bottom) Values of all Members of the Series of 1X-Benzotriazole Derivatives (X= H, CH_3, Cl, NH_2 and OH) in Gas Phase and Aqueous Solution as Functions of Electronegativity of X4 by Using the B3LYP/6-311++G Method**

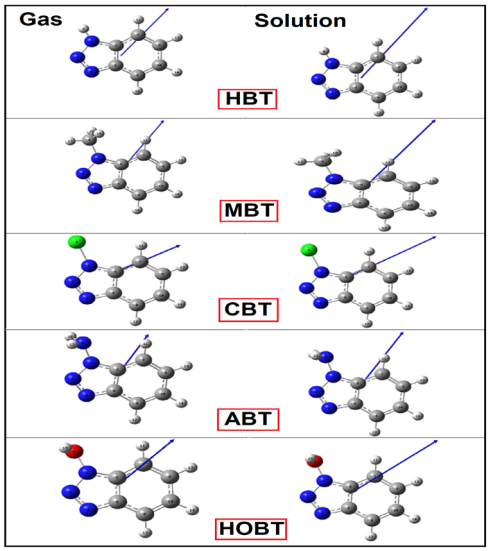

Figure 3. Positions, Orientations and Magnitudes of Dipole Moment Vectors of All Members of the Series of 1X-Benzotriazole Derivatives (X= H, CH3, Cl, NH2 and OH) in Gas Phase and Aqueous Solution by Using the B3LYP/6-311++G Method**

Solvation Energies of all Members of the Series

All members of the series have evidenced changes in the μ values and volumes in aqueous solution and, in particular in the ABT and HOBT derivatives containing donor of H bonds groups, such as the NH_2 and OH groups. Now, the different degrees of hydration of these derivatives are evaluated by means of the solvation energies. This way, from the difference between the corrected solvation energies by ZPVE ($\Delta G_{un}^{\#}$) and by the non-electrostatic terms (ΔG_{ne}) it is possible to calculate the corrected solvation energies (ΔG_c) and (ΔG_{ZPVE}). In Table 3 are summarized the corrected solvation energies by ZPVE and by the total non-electrostatic terms ((ΔG_c) and (ΔG_{ZPVE})) of all members of the series in aqueous solution by using the B3LYP/6-311++G** method.

Table 3. Corrected Solvation Energies ($\Delta G_{C/ZPVE}$) and Uncorrected by ZPVE Energies (ΔG_{un}) and, Volumes Variations (ΔV) for the Series of 1X-Benzotriazole Derivatives (X= H, CH_3, Cl, NH_2, OH) in Gas Phase and Aqueous Solution by Using the B3LYP/6-311++G(d,p) Method. Units Expressed in kJ/mol

B3LYP/6-311++G** Method					
Derivativ	Group	ΔG_{un}	ΔG_{ne}	ΔG_C	$\Delta G_{C/ZPVE}$
HBT	H	-45.11	6.35	-51.46	
		-44.33	6.35		-50.68
MBT	CH_3	-38.03	7.90	-45.93	
		-36.98	7.90		-44.88
CBT	Cl	-27.70	5.77	-33.47	
		-25.18	5.77		-30.95
ABT	NH_2	-41.97	9.97	-51.94	
		-42.23	9.97		-52.20
HOBT	OH	-46.16	12.04	-58.20	
		-45.90	12.04		-57.94

Note: 1-H-benzotriazole (HBT), 1-Methyl-benzotriazole (MBT), 1-Cl-benzotriazole (CBT), 1-Amino-benzotriazole (ABT) and 1-Hidroxy-benzotriazole (HOBT)

In Figure 4 are shown these values as function of electronegativities of X.

Note that both solvation energies present the same variations with the electronegativity and that the HBT derivative has approximately similar values than ABT.

This observation is related to the presence of donor N-H group and of acceptors N atoms in HBT. Thus, as expected ABT and HOBT containing donors of H bonds groups present the most negative (ΔG_c) and (ΔG_{ZPVE}) values which are respectively -51.94/-52.20 and -58.20/-57.94 kJ/mol while the lower values are observed for MBT and CBT.

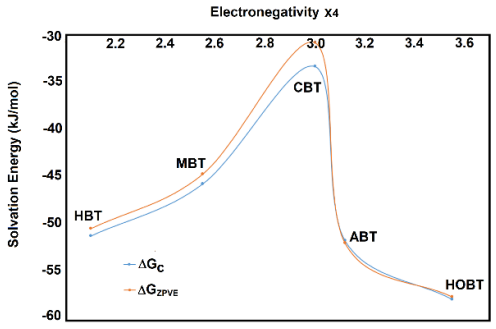

Figure 4. Variations of Solvation Energies of All Members of the Series of 1X-benzotriazole Derivatives (X= H, CH_3, Cl, NH_2 and OH) in Aqueous Solution as Functions of Electronegativity of X4 by Using the B3LYP/6-311++G Method**

The less negative value in MBT is justified because the methyl group is the only hydrophobic of all members of series while the low negative (ΔG_c) and (ΔG_{ZPVE}) values evidenced for CBT only could be justified by the deactivating weak character of Cl atom and, obviously due to its higher size. Comparing these values with reported for antiviral agents, such as amantadine or adamantadine (-23.07 kJ/mol) and rimantadine (-22.78 kJ/mol), all members of the series present higher solvation energy values, that is, most negative values than the antiviral agents (Brandán, 2021; Iramain et al., 2022). These results are interesting because for the quinolone benzotriazole derivative the (ΔG_c) and (ΔG_{ZPVE}) values are respectively -69.72 and -70.29 kJ/mol, higher than antiviral chloroquine (Karrouchi et al., 2023).

Geometrical Parameters of All Members of the Series

The optimized geometrical parameters of all members of the series in gas phase and water are compared with the experimental determined for DD2 and for the 1-Chloro-1*H*-1,2,3-benzotriazole derivative by using X-ray diffraction (Karrouchi et al., 2023; Yuan et al., 2012). The correlations were expressed in terms of root-mean-square deviation values (RMSD). Hence, in Table 4 are presented the bond lengths for the series of 1X-Benzotriazole derivatives (X= H, CH_3, Cl, NH_2, OH) with the corresponding RMSD values while Figure 5 shows the variations in the distances related to triazole and benzyl rings and, to the N1-X4 bonds as function of electronegativities of X4.

Table 4. Comparison of Calculated Geometrical Parameters for the Series of 1X-Benzotriazole Derivatives (X= H, CH_3, Cl, NH_2, OH) in Gas Phase and Aqueous Solution by Using the B3LYP/6-311++G(d,p) Method with the Corresponding Experimental of 5-((1H-benzo[d][1,2,3]triazol-1-yl)methyl)quinolin-8-ol (DD2) and 1-Chloro-1H-1,2,3-benzotriazole

B3LYP/6-311++G** Method[a]							
Parameters	H	CH_3	Cl	NH_2	OH	Exp.[b]	Exp.[c]
Bond lengths (Å)							
N1-N3	1.363	1.363	1.367	1.366	1.351	1.351(5)	1.350
N1-C5	1.364	1.364	1.368	1.365	1.362	1.373(5)	1.360
X1-N4	1.007	1.449	1.699	1.388	1.369	1.442(5)	1.688
N3-N2	1.286	1.288	1.285	1.288	1.293	1.296(6)	1.305
N2-C6	1.380	1.377	1.381	1.381	1.379	1.378(6)	1.376
C5-C7	1.400	1.401	1.398	1.399	1.399	1.389(6)	1.386
C5-C6	1.407	1.408	1.405	1.405	1.407	1.377(6)	1.386
C7-C9	1.385	1.385	1.385	1.384	1.384	1.338(6)	1.371
C6-C8	1.401	1.402	1.401	1.402	1.403	1.411(7)	1.403
C9-C10	1.414	1.415	1.415	1.416	1.416	1.390(7)	1.390
C8-C10	1.383	1.383	1.382	1.382	1.382	1.382(8)	1.371
RMSD[b]	**0.133**	**0.020**	**0.080**	**0.025**	**0.029**		
RMSD[c]	**0.206**	**0.073**	**0.015**	**0.091**	**0.097**		
Aqueous Solution							
N1-N3	1.348	1.350	1.358	1.354	1.342	1.351(5)	1.350
N1-C5	1.361	1.364	1.369	1.364	1.363	1.373(5)	1.360
X1-N4	1.012	1.455	1.699	1.391	1.364	1.442(5)	1.688
N3-N2	1.298	1.301	1.293	1.298	1.301	1.296(6)	1.305
N2-C6	1.378	1.375	1.379	1.378	1.378	1.378(6)	1.376

C5-C7	1.401	1.402	1.398	1.400	1.399	1.389(6)	1.386
C5-C6	1.406	1.406	1.404	1.404	1.405	1.377(6)	1.386
C7-C9	1.383	1.383	1.384	1.383	1.383	1.338(6)	1.371
C6-C8	1.404	1.404	1.403	1.404	1.404	1.411(7)	1.403
C9-C10	1.418	1.418	1.417	1.418	1.418	1.390(7)	1.390
C8-C10	1.382	1.382	1.381	1.382	1.38	1.382(8)	1.371
RMSD[b]	**0.131**	**0.019**	**0.080**	**0.024**	**0.030**		
RMSD[c]	**0.204**	**0.071**	**0.013**	**0.090**	**0.098**		

Note: [a]This work, [b]From Ref (Karrouchi et al., 2023), [c]From Ref (Yuan et al., 2012), Bold letter, RMSD values. 1-H-benzotriazole (HBT), 1-Methyl-benzotriazole (MBT), 1-Cl-benzotriazole (CBT), 1-Amino-benzotriazole (ABT) and 1-Hidroxy-benzotriazole (HOBT).

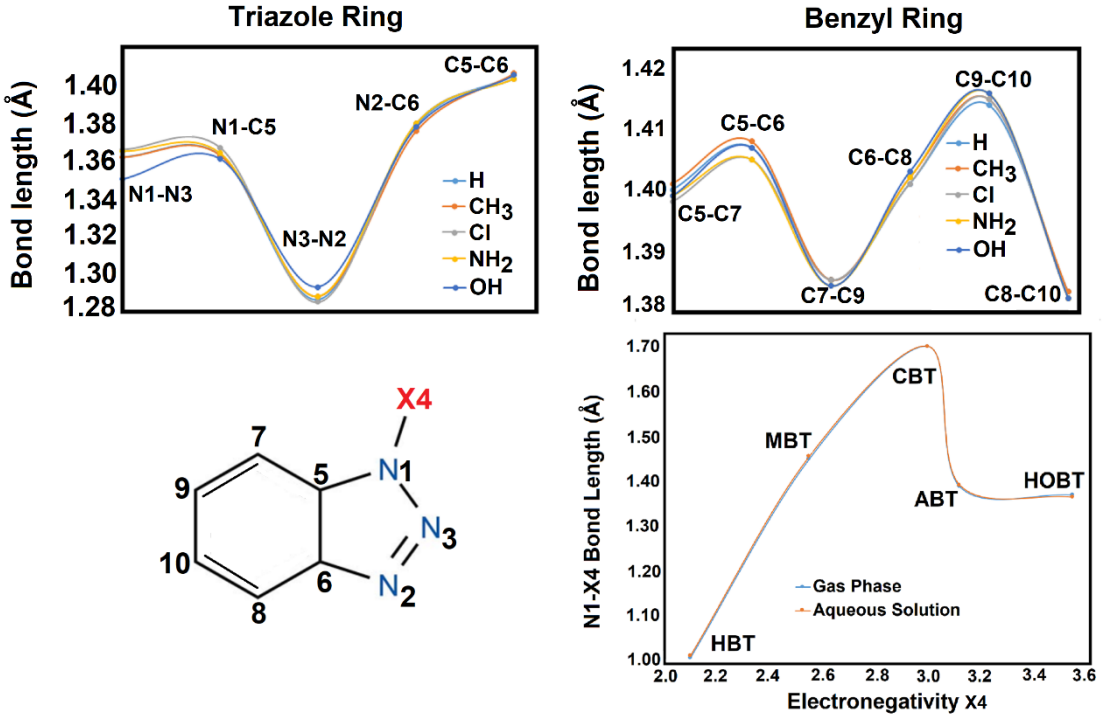

Figure 5. Bonds Lengths of Triazole and Benzyl Rings of All Members of the Series of 1X-Benzotriazole Derivatives (X= H, CH_3, C_l, NH_2 and OH) in Gas Phase and Variations of N1-X4 Bonds as Functions of Electronegativity of X4 by Using the B3LYP/6-311++G Method. Note that a General Structure is Also Presented**

Note that the general structure of all 1-X-benzotriazole derivatives is also presented in the figure. Reasonable concordances are obtained with both structures, thus, RMSD values from 0.133 to 0.019 Å are obtained when the parameters are compared with DD2 while the values change from 0.206 to 0.013 Å when they are compared with the chlorinated derivative (Karrouchi et al., 2023; Yuan et al., 2012). In this latter case, better correlations for CBT are observed because the predicted structure is the same than the experimental compared. Analysing the five bonds of triazole rings we observed that for the five derivatives the N3-N2 bonds have double bonds characters and together with the N1-N3 bonds are the only that slightly change when change X. Thus, the lower N3-N2 and N1-N3 distances are observed for CBT and HBT, respectively. Regarding, the variations of N1-X4 bonds with the

electronegativity it is observed that the lower distance correspond to HBT while the higher to chlorinated derivative, as expected because the Cl atom has deactivating character and higher size, as was mentioned in above sections. If now the bond lengths of benzyl rings are analysed, we observed from Figure 5 that the C7-C9 and C8-C10 bonds have double bonds characters while C5-C7 partial double bonds characters and, finally, C9-C10 have in all derivatives simple bonds characters. Here, the C5-C6, C5-C7 and C9-C10 bonds have different values in all derivatives because they are influenced by the different X groups through the N1-X4 bonds. When the variations of N1-X4 bond lengths of all of members of the series in the two media are graphed as function of polarity N1-X4 bond in Figure S3, we see that, in general, the N1-X4 bond lengths decrease according increase the polarity of bonds. Only a slight difference is observed in MBT than ABT. Hence, this study clearly evidences the effects of electronegativity of X4 and, in particular, of polarity of N1-X4 bonds on the bond lengths involved in both rings and especially on the N1-X4 bonds.

NMR Study

In the section previous, we see the dependence of N1-X4 bonds with the polarity of bonds and now, we must know the correlations between the predicted ^{1}H and ^{13}C-NMR spectra for all members of the series of 1X-Benzotriazole derivatives (X= H, CH_3, Cl, NH_2, OH) in aqueous solution by using the B3LYP/6-311++G(d,p) method. Therefore, in Tables 5 and 6 are summarized the comparisons of predicted ^{1}H- and ^{13}C-NMR chemical shifts for all members of series by using the GIAO and B3LYP/6-311++G** methods. The comparisons are shown in Figure 6 together with the structures and numbering of involved H and C atoms. Figure 6a shows that all H atoms undergoes changes when change the X4 group but the higher chemical shifts are observed in δ_{H11} and δ_{H12} , having δ_{H12} higher values because these atoms are closer to triazole rings while low chemical shifts are observed for the H13 and H14 atoms.

Table 5. Observed and Calculated 1H Chemical Shifts (δ in ppm) for Series of 1X-Benzotriazole Derivatives (X= H, CH_3, Cl, NH_2, OH) in Aqueous Solution by Using the B3LYP/6-311++G(d,p) Method

B3LYP/6-311++G**[a]					
Atoms	HBT	MBT	CBT	ABT	HOBT
4-H	11.00				
11-H	7.59	7.45	7.54	7.73	7.58
12-H	8.30	8.21	8.20	8.17	8.19
13-H	7.53	7.54	7.62	7.55	7.57
14-H	7.45	7.48	7.51	7.45	7.50
15-H		3.83		4.97	5.57
16-H		3.81		4.97	
17-H		4.71			

Note: [a]This work GIAO/B3LYP/6-311++G** Ref. to TMS. 1-H-benzotriazole (HBT), 1-Methyl-benzotriazole (MBT), 1-Cl-benzotriazole (CBT), 1-Amino-benzotriazole (ABT) and 1-Hidroxy-benzotriazole (HOBT)

Table 6. Observed and Calculated ^{13}C Chemical Shifts (δ in ppm) for Series of 1X-Benzotriazole Derivatives (X= H, CH_3, Cl, NH_2, OH) in Aqueous Solution by Using the B3LYP/6-311++G(d,p) method.

B3LYP/6-311++G**[a]					
Atoms	HBT	MBT	CBT	ABT	HOBT
5-C	137.64	138.90	138.80	138.52	133.22
6-C	150.80	152.81	149.75	150.83	149.93
7-C	111.43	110.95	111.55	113.00	110.75
8-C	125.43	125.73	125.82	125.40	126.04
9-C	131.27	130.53	132.70	131.77	131.75
10-C	127.72	127.55	128.08	127.72	128.20

Note: [a]This work GIAO/B3LYP/6-311++G** Ref. to TMS. 1-H-benzotriazole (HBT), 1-Methyl-benzotriazole (MBT), 1-Cl-benzotriazole (CBT), 1-Amino-benzotriazole (ABT) and 1-Hidroxy-benzotriazole (HOBT)

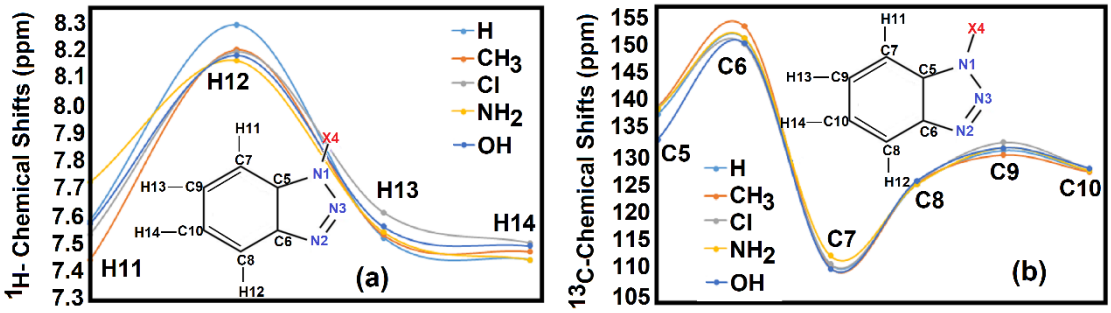

Figure 6. Predicted ^{1}H and ^{13}C-NMR Chemical Shifts (in ppm) for All Members of the Series of 1X-Benzotriazole Derivatives (X= H, CH_3, Cl, NH_2, OH) in Aqueous Solution by Using the B3LYP/6-311++G(d,p) Method

Note that the highest δ_{H12} is observed for HBT (light blue colour) due to that this derivative has the H4 atom with low electronegativity and higher polarity of N1-H4 bond and, in addition the N-H group is donor of H bonds. The highest δ_{H12} is observed for ABT because this derivative has a strong activating NH_2 group and, besides, the group is donor of H bonds. Regarding Figure 6b, we observed that all derivatives show lower δ_{C7} values and higher δ_{C6} values, having the HOBT derivative the lower δ_{C6} and δ_{C7} values. Here, the strong activating character of OH and the higher electronegativity justify such observations. The δ_{C5} and δ_{C9} slightly change with the derivative while δ_{C8}, and δ_{C10} present similar values in all derivatives. This study evidence that ^{1}H-NMR chemical shifts in all derivatives are strongly influenced by the electronegativity, the activating character of X group and the polarity of N1-X4 bond while ^{13}C-NMR chemical shifts only by the electronegativity and activating character of X group.

Atomic Charges, MEP and Bond Orders

Previous studies have shown the effects of different X4 groups on dipole moments, volumes, solvation energies, bond lengths and ^{13}C-NMR chemical shifts of all of members of series of 1-X-benzotriazole derivatives. In this section, the Merz-Kollman (MK) and natural population atomic (NPA) charges and molecular electrostatic potentials (MEP) and bond orders

(BO) have been calculated to analyse the modifications of these parameters and, in particular, with the atoms of triazole rings (N1, N2, N3 and X4). Hence, in Table S1 are summarized the MK and NPA charges, MEP and bond orders, expressed as Wiberg indexes for all members of the series of 1X-Benzotriazole derivatives (X= H, CH_3, Cl, NH_2, OH) in gas phase and aqueous solution by using the B3LYP/6-311++G(d,p) method. Figure 7 shows the variations of calculated MK and NPA charges on N1, N2, N3 and X4 for all derivatives in both media by using the B3LYP/6-311++G** method. First, it is observed that the NPA charges on four atoms in both media don't change while the MK changes on N1 and X4 of HBT, MBT and HOBT derivatives show sligth changes in solution.

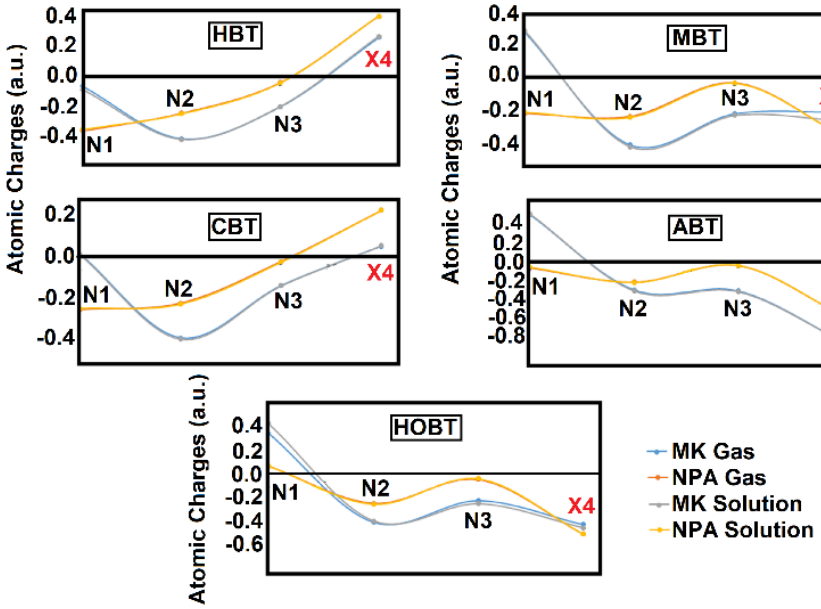

Figure 7. Atomic MK and NPA Charges of all Members of the Series of 1X-Benzotriazole Derivatives (X= H, CH_3, C_l, NH_2 and OH) in Gas Phase and Aqueous Solution by Using the B3LYP/6-311++G Method**

Note that only HBT and CBT present positive MK and NPA charges on X4 because when X4 is H the N1-H4 bond shows a higher polarity (both charges have negative signs) while in CBT the polarity is nulla and the Cl evidence a weak deactivating character. On the other hand, positive MK charges on N1 of HBT, ABT and HOBT derivatives are observed due to that the MK and NPA charges on X4 in these species have negative signs. The MK charges on N2 in all derivatives have lower values, with exception of ABT. When the variations of MK and NPA charges on X4 atoms of all of members of the series of 1-X-benzotriazole derivatives in both environments are analysed as function of electronegativity of X4 by using the B3LYP/6-311++G(d,p) method (Figure S4) we observed positive signs in both charges only for HBT and CBT and the lowest negative value for ABT probably due to the less negative and most positive MK charges on X4 and N1, respectively. The evaluation of MEPs values from Table S1 on the N and X4 atoms in the two media shows only differences on X4, as expected because in all derivatives this atom changes. Thus, when these MEPs values only for X4 are graphed as function of electronegativity of groups from Figure S5, the tendency observed is: HBT < MBT < ABT < HOBT, where the CBT derivative has the less negative value due to Cl atom which has higher MEP. Note that all MEPs present similar values in both environments. When the mapped MEP surfaces for all members of series of 1-X-benzotriazole derivatives with X= H, CH_3, Cl, NH_2 and OH in gas phase are shown in Figure S6 it is observed

changes in colorations on some atoms and the energies of surfaces show the following tendency: 0.0730 (HOBT) > 0.0687 (HBT) > 0.0564 (MBT) > 0.0536 (ABT) > 0.0482 (CBT) a.u. Hence, a certain tendency of MEP energies with the polarity of N1-X4 bond it is observed because HBT (0.9) > HOBT (0.5) = MBT (0.5) > ABT (0.0) = CBT (0.0). The red colorations in all derivatives are observed on the acceptors N atoms because they are nucleophilic sites while the blue colours on the donors N-H, NH_2 and OH ones.

When the bond orders (BO) totals by atom, expressed as Wiberg bond index are analysed from Table S1, it is observed that the N2 and N3 atoms for all species have lower values, as expected because they have double bond character while if the variations of N1-X4 bond orders of all of members of the series in both media are evaluated as function of electronegativity of X4 from Figure S7, we can see that HBT and CBT present the lower values while MBT and ABT the higher ones. Hence, an expected result is obtained because in sections previous we see that the Cl atom produces an enlargement of N1-Cl in CBT due to its weak deactivating character and, this way, a lower BO is expected in this derivative. Possibly, the activating character (AC) of group generate a decreasing in the BOs of the same because $AC_{CH3} < AC_{NH2} = AC_{OH}$. Thus, $BO_{CH3} > BO_{NH2} > BO_{OH}$.

NBO and AIM Calculations

Stabilization energies due to different transitions are expected in these series of 1-X-benzotriazole derivatives because in the structures of some of them we can see donors (N-H, NH_2 and OH) and in all them acceptors (N atoms) groups, and, for these reasons, NBO and AIM calculations were performed for all species by using the NBO 3.1 and AIM 2000 programs (Glendening et al., 1996; Bader, 1990; Biegler-Köning et al., 2001). Thus, in the study by using NBO calculations, the donor-acceptor energy interactions *E(2)* are computed with the Second-Order Perturbation Theory Analysis of Fock Matrix in NBO Basis by using B3LYP/6-311++G** calculations. These main delocalization's energies for all derivatives in both environments are shown in Table S2 while in Figure S8 we can see the variations of these energies with the different groups. From Table S2, all derivatives present three different types of interactions, which are: $\pi \rightarrow \pi^*$, $n \rightarrow \pi^*$ and $\pi^* \rightarrow \pi^*$ transitions while only for ABT an additional $n \rightarrow \sigma^*$ transition is observed while in the CBT and HOBT derivatives other different $\pi^*C5\text{-}C6 \rightarrow \pi^*C7\text{-}C9$ transitions are observed in both media for the first derivative and only in gas phase for the other one. The evaluation of total energy show that CBT in the two media present the higher ΔE_{total} values. This way, probably the total energy values of interactions explain the lower BOs observed from the above study for CBT. Here, we see that the high values observed for ABT and HOBT in gas phase drastically diminishing in solution because both derivatives could be hydrated in this medium due to its acceptors and donor's H bonds groups.

If now the AIM 2000 program is used to calculate the topological properties for all derivatives we see from Figure S9 that there are not bond critical points (BCPs) or intramolecular interactions and, for these reasons, only the electron density and the Laplacian values are calculated in the ring critical points (RCPs) (Bader, 1990; Biegler-Köning et al., 2001). Hence, these results for the series of derivatives are presented in Table S3. Interesting results are observed when the variations of electronic densities of triazole and benzyl ring are graphed as function of electronegativity of X4 in Figure 8.

Hence, the electronic densities of both ring increase with the increase in the electronegativity, with exception of CBT derivative because its values increase in the triazole ring but decrease for the benzyl ring in both media. Thus, for the triazole and benzyl rings, the tendency observed is: HBT < MBT< ABT < HOBT. Here, the effect of electronegativity of CBT is observed on electronic densities of benzyl rings in both media while the OH group increases the electronic densities of triazole rings. Both NBO and AIM studies reveal the strong influence of OH and Cl groups on properties of triazole and benzyl

rings, respectively and, hence on the HOBT and CBT derivatives.

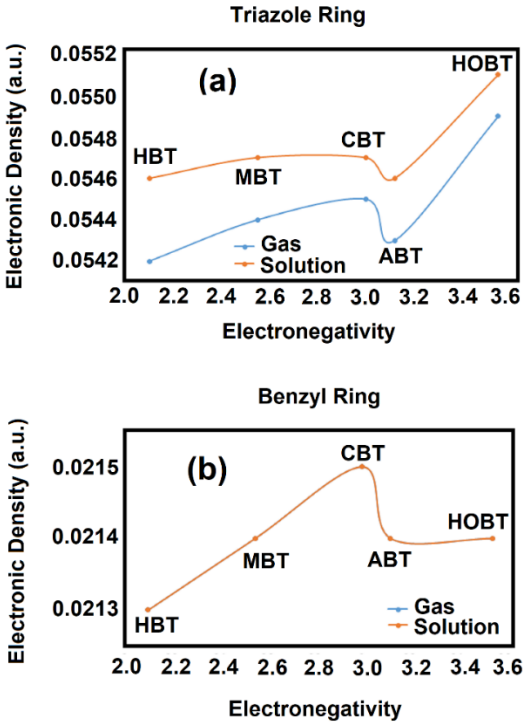

Figure 8. Electronic Densitiy of Triazole and Benzyl Rings of All Members of the Series of 1X-benzotriazole Derivatives (X= H, CH_3, C_l, NH_2 and OH) in Gas Phase and Aqueous Solution as Functions of Electronegativity of X4 by Using the B3LYP/6-311++G Method**

Frontier orbitals studies

Studies and analyses of frontier orbitals are very important in all studied series of benzotriazole derivatives because these factors predict reactivities and behaviours of these species in the two studied media. Thus, the gap values calculated from the differences between the HOMO-LUMO are used to compute different descriptors (Parr & Pearson, 1983; Brandán, 2021; Iramain et al., 2022). Hence, the chemical potential (μ), electronegativity (χ), global hardness (η), global softness (S) and global electrophilicity index (ω) descriptors together with the gap values are shown in Table S4. The equations used are also presented and the table. If the variations of gap values of all of members of the series of 1-X-benzotriazole derivatives are evaluated as function of electronegativity of X4 we can see from Figure S10 that CBT presents the lower values in both media. Thus, the Cl increase the reactivity of CBT in both media while the OH increase the reactivity of HOBT in gas phase but it decreases in water. When the descriptors are analysed from Table S4 and, in particular, the global electrophilicity indexes (ω) for all derivatives are graphed as function of electronegativity of X4 in Figure S11, it is observed that CBT present the higher values in both media while MBT the lower ones. Hence, a higher (ω) in CBT justify its higher reactivity.

Analysing forms, electronic distributions and participations of orbitals from Figure S12 (only presented in gas phase because they are similar in solution) it is observed that both frontier orbitals are mainly localized on the benzotriazole rings, indicating that the HOMO–LUMO are mostly the p-antibonding-type orbitals and, for these reasons, probably the gaps show approximately similar values.

Vibrational study

All series of 1-X-benzotriazole derivatives have been optimized by B3LYP/6-311++G** calculations with C_l symmetry and due to the different number of atoms present in their structures, the number of vibration modes are also different. Thus, HBT and CBT have 14 atoms and, hence, 36 vibration modes are expected; in HOBT with 15 atoms, 39 vibration modes; ABT with 16 atoms, 42 vibration modes and, MBT with 17 atoms 45 vibration modes. Complete assignments were obtained for all derivatives by using the harmonic force fields, transferable scaling factors and normal internal coordinates taking PED contributions ≥ 10% (Pulay et al., 1983; Rauhut & Pulay, 1995; Sundius, 2002). Thus, in Table 7 (Appendix 2) are summarized observed and calculated wavenumbers and assignments for all series of 1X-Benzotriazole derivatives (X= H, CH_3, Cl, NH_2, OH) in the gas phase by using B3LYP/6-311++G** calculations. The predicted IR spectra for all of members of series can be seen in Figure 9 while Figure S13 shows the variations of main stretching modes of both rings with the electronegativity of X. Figure 9 shows clearly in

the higher wavenumbers region (4000-2000 cm^{-1}) the expected strong IR band due to N1-H4 (HBT), N1-CH_3 (MBT), N-NH_2 (ABT) and N1-OH (HOBT) stretching modes while from figure S13 we can see that the N1-Cl4 stretching (ν) mode of CBT is predicted to 417 cm^{-1}, that is at lower wavenumbers than ABT and HOBT. The νN1-C5 and νN1-N3 modes evidence few changes with the group showing greater changes νN1-C5. Evaluating only the most intense bands observed from the 2000-70 cm^{-1} region, the SQM calculations show for HBT two intense bands at 1293 and 450 cm^{-1} which are respectively assigned to νN2-N3 and to N1-H1 out-of-plane deformation mode (γ). For MBT, the bands at 1477, 975 and 746 cm^{-1} which are assigned to νN1-C5 and νN1-N3 and to γC-H, as detailed in Table 7 (Appendix 2). In CBT, the intense bands at 1291, 1041 and 773 cm^{-1} are assigned respectively to νN2-N3, to a deformation triazole ring (βR_1(A2)) and νC-C. For ABT, the intense bands at 1295, 1039 and 756 cm^{-1} are assigned to νN2-N3, νN1-N3 and γC-H. Finally, for HOBT the intense bands located at 1272, 1052, 750 and 190 cm^{-1} are assigned to OH deformation, νN1-N3, γC-H and torsion τOH modes, respectively. These analyses evidence in clear from the different intensities and positions of vibration modes related to N1-X4 group.

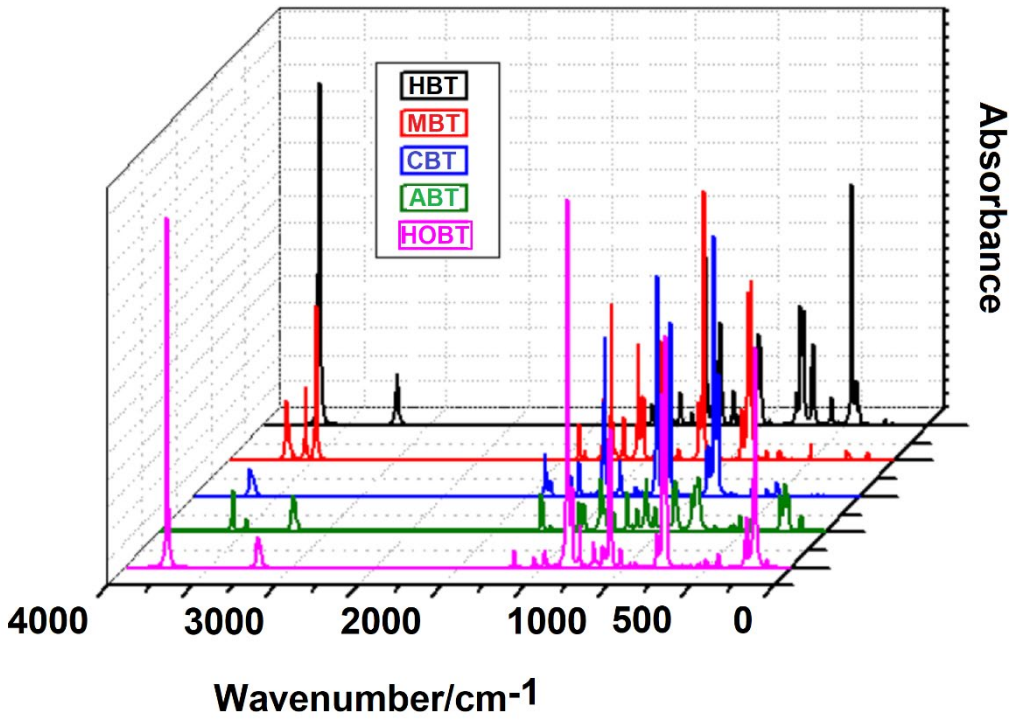

Figure 9. Predicted Infrared Spectra of All Members of the Series of 1X-Benzotriazole Derivatives (X= H, CH_3, C_l, NH_2 and OH) in Gas Phase by Using the Hybrid B3LYP/6-311++G Method**

Force Constants

Scaled force constants for all members of the series of 1X-Benzotriazole derivatives were obtained from the harmonic force fields with the SQMFF methodology and the Molvib program (Pulay et al., 1983; Rauhut & Pulay, 1995; Sundius, 2002). Table 8 (Appendix 2) shows the values of these constants for all members of

series while in Figure S14 are presented the variations of these constants as function of electronegativity of X4.

Quickly, the analyses from the graphics show that the $f(\nu C\text{-}H)_{A1}$ and $f(\nu C\text{-}C)_{A1}$ force constants related to A1 benzyl rings are practically the same for all members of series indicating that they are not influenced by X4 while the higher changes are expected in the $f(\nu N1\text{-}X4)$ force constants due to the presences of CH_3 and Cl in MBT and CBT, respectively, as was observed from vibrational study. Then, slight changes are also observed in the $f(\nu C\text{-}N)_{A2}$ $f(\nu N\text{-}N)_{A2}$ force constants due to the presence of acceptors N atoms in the triazole rings (A2) of all derivatives. Such changes indicate the effect of X4 on C-N and N-N bonds of triazole rings.

Electronic spectra

The effect of X4 on the positions and intensities of two bands observed in the predicted electronic spectra for all members of series in aqueous solution have been also studied by using the B3LYP/6-311++G** method. Figure 10 shows the five spectra for all members of series benzotriazole in aqueous solution while in Table 9 are summarized the positions, intensities and assignments of two bands (I and II) observed in the electronic spectra of all members of the series of 1-X-Benzotriazole derivatives in aqueous solution.

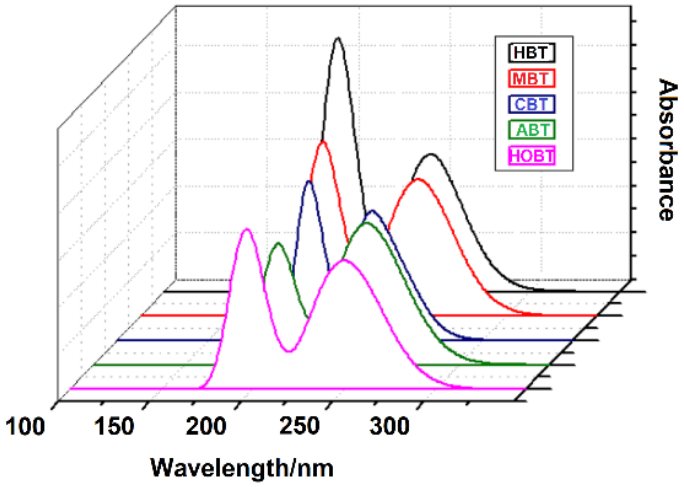

Figure 10. Predicted Electronic Spectra of All Members of the Series of 1X-Benzotriazole Derivatives (X= H, CH3, Cl, NH2 and OH) in Gas Phase by Using the Hybrid B3LYP/6-311++G Method**

Table 9. Positions (in nm), Intensities and Assignments of Two Bands Observed in the Electronic Spectra of All Members of the Series of 1-X-Benzotriazole Derivatives (X= H, CH_3, C_l, NH_2, OH) in Aqueous Solution by Using the B3LYP/6-311++G(d,p) Method

Derivatives	B3LYP/6-311++G** Method[a]		
	Band I	Band II	Assignments
HBT	240.5 (s), f=0.1012	194.3 (vs), f= 0.0012	$\pi\rightarrow\pi^*$, $n\rightarrow\pi^*$, $\pi^*\rightarrow\pi^*$
MBT	253.5 (s), f= 0.0032	199.8 (vs), f= 0.1646	$\pi\rightarrow\pi^*$, $n\rightarrow\pi^*$, $\pi^*\rightarrow\pi^*$
CBT	242.4 (s), f= 0.0088	194.8 (vs), f= 0.1352	$\pi\rightarrow\pi^*$, $n\rightarrow\pi^*$, $\pi^*\rightarrow\pi^*$
ABT	243.4 (vs), f= 0.1098	201.5 (s), f= 0.1017	$\pi\rightarrow\pi^*$, $n\rightarrow\pi^*$, $\pi^*\rightarrow\pi^*$, $n\rightarrow\sigma^*$
HOBT	254.8 (s), f= 0.0044	193.7 (vs), f= 0.0040	$\pi\rightarrow\pi^*$, $n\rightarrow\pi^*$, $\pi^*\rightarrow\pi^*$

Note: [a]This work, f= Oscillator strength, s= strong, vs= very strong.

Figure S15 shows the variations in positions of two bands as function of electronegativity of X4. In both Figures 10 and S15 and, in Table 9 are observed that in all members of series the intensities of bands I are higher than the corresponding to II, with exception of ABT, where the band I has higher intensity than the II one. Thus, the higher intensity of band II in ABT is related to additional $n \rightarrow \sigma^*$ interaction observed as a consequence of N1-N4 bond, as supported by NBO calculations. Both bands are assigned to $\pi \rightarrow \pi^*$, $n \rightarrow \pi^*$ and $\pi^* \rightarrow \pi^*$ transitions as predicted by NBO calculations. These shifting of bands observed in the electronic spectra for the different derivatives show the effects of X4 groups on the positions of UV bands.

Conclusions

The following conclusions were obtained from this investigation:

- The polarity of the N1-X4 bonds and the hydrophilic and/or donor/acceptor character of X4 have influence on dipole moments and volumes of all members of series.

- The electronegativities of different X4 groups and the polarity of N1-X4 bonds evidence clear effects on the bond lengths involved in both rings and especially on the N1-X4 bonds. Thus, the N1-X4 bond lengths increase from N1-H4 to N1-Cl4 according decrease the polarity of bond: N1-H4 > N1-C4 = N1-O4 > N1-Cl4 = N1-N4.

- The ^{1}H-NMR chemical shifts in all derivatives are strongly influenced by the electronegativity, the activating character of X group and the polarity of N1-X4 bond while ^{13}C-NMR chemical shifts only by the electronegativity and activating character of X group.

- A certain tendency in the MEP energies with the polarity of N1-X4 bond it is observed because HBT (0.9) > HOBT (0.5) = MBT (0.5) > ABT (0.0) = CBT (0.0). The red colorations in all derivatives are observed on the acceptors N atoms because they are nucleophilic sites while the blue colours on the donors N-H, NH_2 and OH ones.

- NBO calculations suggest that CBT in the two media present the higher ΔE_{total} values while the high values observed for ABT and HOBT in gas phase drastically diminishing in solution due to that both derivatives could be hydrated in this medium because they have acceptors and donor's H bonds groups.

- The electronic densities of both rings increase with the increase in the electronegativity of X4, with exception of CBT derivative because its values increase in the triazole ring but decrease for the benzyl ring in both media. Thus, for the triazole and benzyl rings, the tendency observed is: HBT < MBT< ABT < HOBT. Here, the effect of electronegativity of Cl on electronic densities of both rings is clearly observed in the derivative CBT.

- Both NBO and AIM studies reveal the strong influence of Cl on properties of both rings and, on the CBT derivative.

- The Cl increase the reactivity of CBT in both media probably due to its higher (ω) while the OH increase the reactivity of HOBT in gas phase but it decreases in water. Hence, the higher reactivity is observed for CBT.

- The determinations of harmonic force fields and the vibrational analyses for all of members of series have evidenced very good correlations between the stretching force constants and their respective assignments.

Availability of data

All data generated or analysed during this study are included in this published article.

CRediT authorship contribution statement

María E. Manzur: Conceptualization, Methodology. Maximiliano A. Iramain: Data curation. Vahidreza Darugar: Conceptualization, Methodology. Mohammad Vakili: review,

editing. Silvia Antonia Brandán: Write original draft preparation, editing, supervision review.

Supplementary Information

Figures S1-S15 (Appendix 1) and TablesS1-S4 (Appendix 2).

Acknowledgements

This work was supported with grants from CIUNT Project N°. 26/D714 (Consejo de Investigaciones, Universidad Nacional de Tucumán) and by Ferdowsi University of Mashhad, Iran. The authors would like to thank Prof. Tom Sundius for his permission to use MOLVIB.

References

Asimakopoulos, A.G., Wang, L., Thomaidis, N.S. & Kannan, K. (2013). Benzotriazoles and benzothiazoles in human urine from several countries: A perspective on occurrence, biotransformation, and human exposure. *Environmental International, 59*, 274-281. https://doi.org/10.1016/j.envint.2013.06.007

Bader, R.F.W. (1990). *Atoms in Molecules, A Quantum Theory*. Oxford: Oxford University Press.

Becke, A.D. (1988). Density-functional exchange-energy approximation with correct asymptotic behavior. *Physical Review A, 38*, 3098-3100. https://doi.org/10.1103/physreva.38.3098

Besler, B.H., Merz Jr, K.M. & Kollman, P.A. (1990). Atomic charges derived from semiempirical methods. *Journal of Computational Chemistry, 11*, 431-439. ttps://doi.org/10.1002/jcc.540110404

Biegler-Köning, F., Schönbohm, J. & Bayles, D. (2001). AIM 2000. A Program to Analyze and Visualize Atoms in Molecules. *Journal of Computational Chemistry, 22*, 545. https://doi.org/10.1002/1096-987X(20010415)22:5<545::AID-JCC1027>3.0.CO;2-Y

Brandán, S.A. (2021). Normal internal coordinates Force fields and vibrational study of Species Derived from Antiviral adamantadine, *International Journal of Quantum Chemistry, 121*(2), e26425. https://doi.org/10.1002/qua.26425

Chen, R., Guo, L. & Xu, S. (2014). Experimental and Theoretical Investigation of 1-hydroxybenzotriazole as a Corrosion Inhibitor for Mild Steel in Sulfuric Acid Medium. *International Journal of Electrochemical Science, 9*(12), 6880-6895. https://doi.org/10.1016/S1452-3981(23)10938-2

Darugar, V., Vakili, M., Brandán, S. & Adli, S. (2023). Electronic transport on the two state "ON–OFF" of 1,3,3-trimethylindolino-6'-nitrobenzopyrylospiran as a light-driven molecular optical switch: A first-principle study. *Journal of Molecular Graphics and Modelling, 120*, 108420. https://doi.org/10.1016/j.jmgm.2023.108420

Ditchfield, R. (1974). Self-consistent perturbation theory of diamagnetism. I. A gage-invariant LCAO (linear combination of atomic orbitals) method for NMR chemical shifts. *Molecular Physics, 27,* 714–722. http://dx.doi.org/10.1080/00268977400100711

Emoto, C., Murase, S., Sawada, Y., Jones, B.C. & Iwasaki, K. (2003). In Vitro Inhibitory Effect of 1-Aminobenzotriazole on Drug Oxidations Catalyzed by Human Cytochrome P450 Enzymes: A Comparison with SKF-525A and Ketoconazole. *Drug Metabolism and Pharmacokinetics, 18*(5), 287-295. https://doi.org/10.2133/dmpk.18.287

Finšgar, M. & Milošev, I. (2010). Inhibition of copper corrosion by 1,2,3-benzotriazole: A review. *Corrosion Science, 52*(9), 2737-2749. https://doi.org/10.1016/j.corsci.2010.05.002

Frisch, M.J., Trucks, G.W., Schlegel, H.B., Scuseria, G.E., Robb, M.A., Cheeseman, J.R., … & Petersson, G.A. (2009). *Gaussian 09. Revision A.02*. Wallingford CT: Gaussian Inc.

Glendening, E.D., Badenhoop, J.K., Reed, A.D.,

Carpenter, J.E. & Weinhold, F. (1996). *NBO 3.1*. Theoretical Chemistry Institute, University of Wisconsin. Madison, WI.

Gupta, V.P. (2016). *Principles and Applications of Quantum Chemistry*. Chapter 12: Characterization of Chemical Reactions. India: Elsevier Inc. https://doi.org/10.1016/B978-0-12-803478-1.00012-1

Hirai, H., Shibata, H., Kawai, S. & Nishida, T. (2006). Role of 1-hydroxybenzotriazole in oxidation by laccase from Trametes versicolor. Kinetic analysis of the laccase-1-hydroxybenzotriazole couple. *FEMS Microbiology Letters, 265,* 56–59. https://doi.org/10.1111/j.1574-6968.2006.00474.x

Iramain, M.A., Ruiz Hidalgo, J., Sundius, T. & Brandán, S.A. (2022). A Combined Study on Structures and Vibrational Spectra of Antiviral Rimantadine using SQMFF and DFT calculations. *Heliyon, 8*, e10102. https://doi.org/10.1016/j.heliyon.2022.e10102

Karrouchi, K., Himmi, B., Brandán, S.A., Sert, Y., Kawther, A.A., Dege, N., Cinar, E.B., El Louzi, A. & Bougrin, K. (2023). A quinoline-benzotriazole derivative: Synthesis, crystal structure and characterization by using spectroscopic, DFT and molecular docking methods. *Results in Chemistry, 5*, 100916. https://doi.org/10.1016/j.rechem.2023.100916

Kokalj, A., Peljhan, S., Finšgar, M. & Milošev, I. (2010). What Determines the Inhibition Effectiveness of ATA, BTAH, and BTAOH Corrosion Inhibitors on Copper? *Journal of the American Chemical Society*, *132*(46), 16657–16668. https://doi.org/10.1021/ja107704y

Kotowska, U., Struk-Sokołowska, J. & Piekutin, J. (2021). Simultaneous determination of low molecule benzotriazoles and benzotriazole UV stabilizers in wastewater by ultrasound-assisted emulsification microextraction followed by GC–MS detection *Scientific Reports, 11*, 10098. https://doi.org/10.1038/s41598-021-89529-1

Lee, C., Yang, W. & Parr, R.G. (1988). Development of the Colle-Salvetti correlation-energy formula into a functional of the electron density. *Physical Review B, 37*, 785-789. https://doi.org/10.1103/physrevb.37.78

Malow, M., Klaus, D. & Neuenfeld, W.S. (2007). On the explosive properties of 1*H*-benzotriazole and 1*H*-1,2,3-triazole. *Tetrahedron Letters, 48*(7), 1233-1235. https://doi.org/10.1016/j.tetlet.2006.12.046

Marenich, A.V., Cramer, C.J. & Truhlar, D.G. (2009). Universal solvation model based on solute electron density and a continuum model of the solvent defined by the bulk dielectric constant and atomic surface tensions. *Journal of Physical Chemistry, B113*, 6378-6396. https://doi.org/10.1021/jp810292n

Miertus, S., Scrocco, E. & Tomasi, J. (1981). Electrostatic interaction of a solute with a continuum. *Chemical Physics, 55,* 117-129. https://doi.org/10.1016/0301-0104(81)85090-2

Mugford, C.A., Mortillo, M., Mico, B.A. & Tarloff, J.B. (1992). 1-Aminobenzotriazole-induced destruction of hepatic and renal cytochromes P450 in male Sprague-Dawley rats. *Fundamental and Applied Toxicology, 19*(1), 43-49. https://doi.org/10.1016/0272-0590(92)90026-e

Nielsen, A.B. & Holder, A.J. (2008). *Gauss View 5.0, User's Reference*. Pittsburgh, PA: GAUSSIAN Inc.

Ortiz de Montellano, P.R. (2018). 1-Aminobenzotriazole: A Mechanism-Based Cytochrome P450 Inhibitor and Probe of Cytochrome P450 Biology. Medicinal Chemistry, 8(3), 1-73. https://doi.org/10.4172/2161-0444.1000495

Pacheco-Juárez, J., Montesdeoca-Esponda, M., Torres-Padrón, M.E., Sosa-Ferrera, Z. & Santana-Rodríguez, J.J. (2019). Analysis and occurrence of benzotriazole ultraviolet stabilisers in different species of seaweed. *Chemosphere, 236*, 124344. https://doi.org/10.1016/j.chemosphere.2019.124344

Parr, R.G. & Pearson, R.G. (1983). Absolute hardness: companion parameter to absolute electronegativity. *Journal of American Chemical*

Society, 105, 7512-7516. https://doi.org/10.1021/ja00364a005.

Parrish, K.E., Mao, J., Chen, J., Jaochico, A., Ly, J., Ho, Q., Mukadam, S. & Wright, M. (2015). In vitro and in vivo characterization of CYP inhibition by 1-aminobenzotriazole in rats. *Biopharmaceutics & Drug Disposition, 37*(4), 200-211. https://doi.org/10.1002/bdd.2000

Pulay, P., Fogarasi, G., Pongor, G., Boggs, J.E. & Vargha, A. (1983). Combination of theoretical ab initio and experimental information to obtain reliable harmonic force constants. Scaled quantum mechanical (QM) force fields for glyoxal, acrolein, butadiene, formaldehyde, and ethylene. *Journal of American Chemical Society, 105*, 7073. https://doi.org/10.1021/ja00362a005

Rauhut, G. & Pulay, P. (1995). Transferable scaling factors for density functional derived vibrational force fields. *Journal of Physical Chemistry, 99*, 3093–3099. https://doi.org/10.1021/j100010a019

Santiago, M.R., Coimbra, R., Escapa, C. & Otero, M. (2018). Treatment of dairy wastewater by oxygen injection: Occurrence and removal efficiency of a benzotriazole based anticorrosive. *Water, 10*, 155-168. https://doi.org/10.3390/w10020155

Shaik, A.N., LeDuc, B.W. & Khan, A.A (2017). Characterization of 1-Aminobenzotriazole and Ketoconazole as Novel Inhibitors of Monoamine Oxidase (MAO): An In Vitro Investigation. *European Journal of Drug Metabolism and Pharmacokinetics, 42*(5), 827-834. https://doi.org/10.1007/s13318-017-0401-6

Shi, Z.-Q., Liu, Y.-S., Xiong, Q., Cai, W.-W. & Ying, G.-G. (2019). Occurrence, toxicity and transformation of six typical benzotriazoles in the environment. A review. *Science of the Total Environment, 661*, 407-421. https://doi.org/10.1016/j.scitotenv.2019.01.138

Sun, Q., Harper, T.W., Dierks, E.A., Zhang, L., Chang, S., Rodrigues, A.D. & Marathe, P. (2011). 1-Aminobenzotriazole, a known cytochrome P450 inhibitor, is a substrate and inhibitor of N-acetyltransferase. *Drug Metabolism and Disposition, 39*(9), 1674-1679. https://doi.org/10.1124/dmd.111.039834

Sundius, T. (2002). Scaling of ab initio force fields by MOLVIB. Vibrational Spectroscopy, 29, 89-95. https://doi.org/10.1016/S0924-2031(01)00189-8

Tomasi, J., & Persico, J. (1994). Molecular Interactions in Solution: An Overview of Methods Based on Continous Distributions of the Solvent. *Chemical Review, 94*, 2027-2094. https://doi.org/10.1021/cr00031a013

Ugliengo, P. (1998). *MOLDRAW Program.* University of Torino, Dipartimento Chimica IFM, Torino, Italy.

Vemula, P.K., Ganguly, B. & Bhattacharya, S. (2005). Computational Study on Hydroxybenzotriazoles as Reagents for Ester Hydrolysis. *The Journal of Organic Chemistry, 69*(25), 8634-8642. https://doi.org/10.1021/jo049539w

Watanabe, A., Mayumi, K., Nishimura, K. & Osaki, H. (2016). In vivo use of the CYP inhibitor 1-aminobenzotriazole to increase long-term exposure in mice. *Biopharmaceutics & Drug Disposition, 37*(6), 373-378. https://doi.org/10.1002/bdd.2020

Wehrstedt, K.D., Wandrey, P.A. & Heitkamp, D. (2005). Explosive properties of 1-hydroxybenzotriazoles. *Journal of Hazardous Materials, 126*(1-3), 1-7. https://doi.org/10.1016/j.jhazmat.2005.05.044

Yuan, M.Y., Zhao, X. & Zheng, L.L. (2012). 1-Chloro-1*H*-1,2,3-benzotriazole. *Acta Crystallographica, E68*, o3432. https://doi.org/10.1107/S1600536812044820

Appendix 1

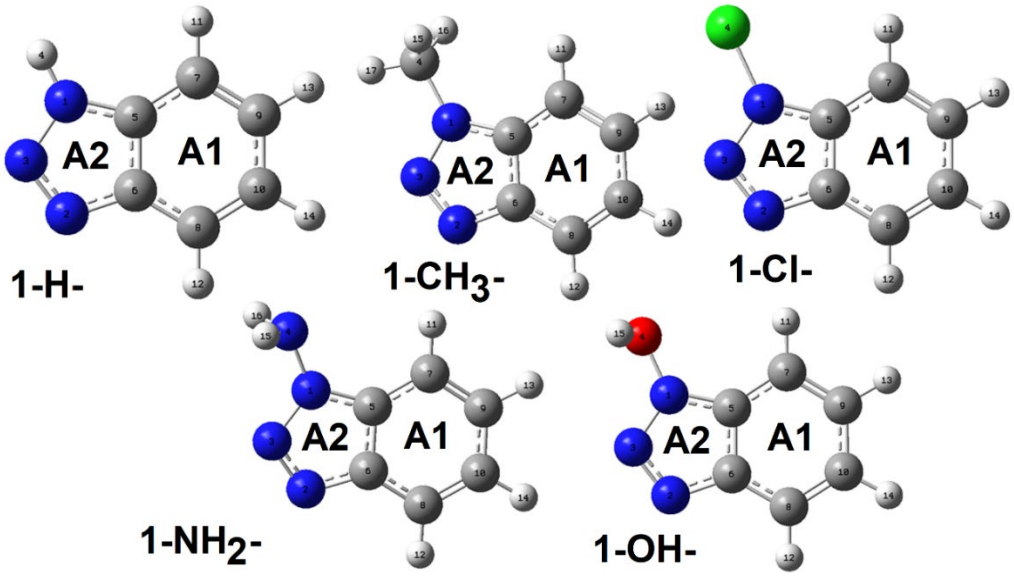

Figure S1. Optimized Structures of Series of 1-X-Benzotriazole Derivatives with X= H, CH_3, C_l, NH_2, and OH in Gas Phase with the Atoms Labelling and the Identifications of All Rings by Using the B3LYP/6-311++G(d,p) Method

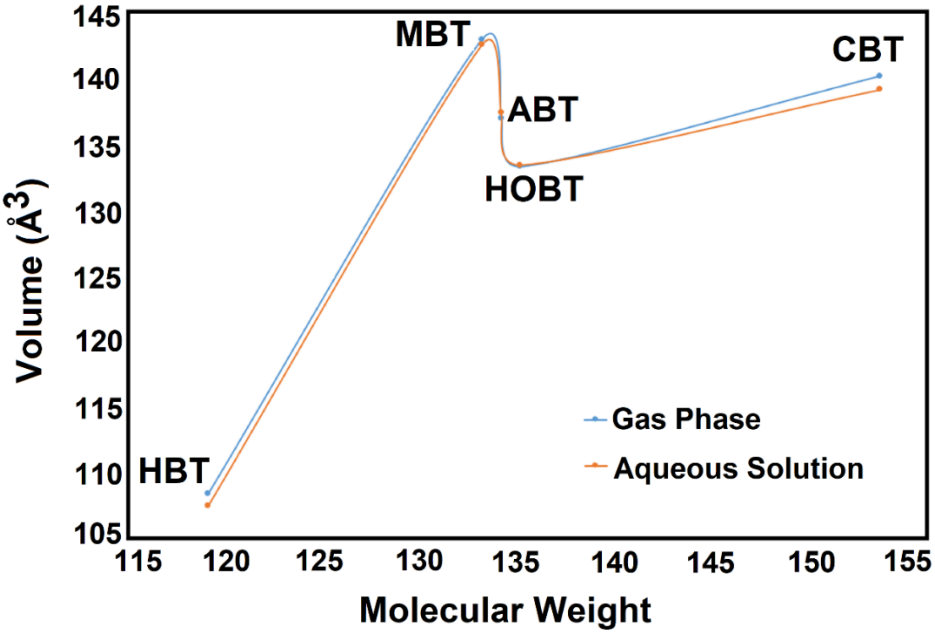

Figure S2. Variations Volumes of All of Members of the Series of 1-X-Benzotriazole Derivatives with X= H, CH_3, C_l, NH_2, and OH in Gas Phase and Aqueous Solution as Function of Molecular Weights by Using the B3LYP/6-311++G(d,p) Method

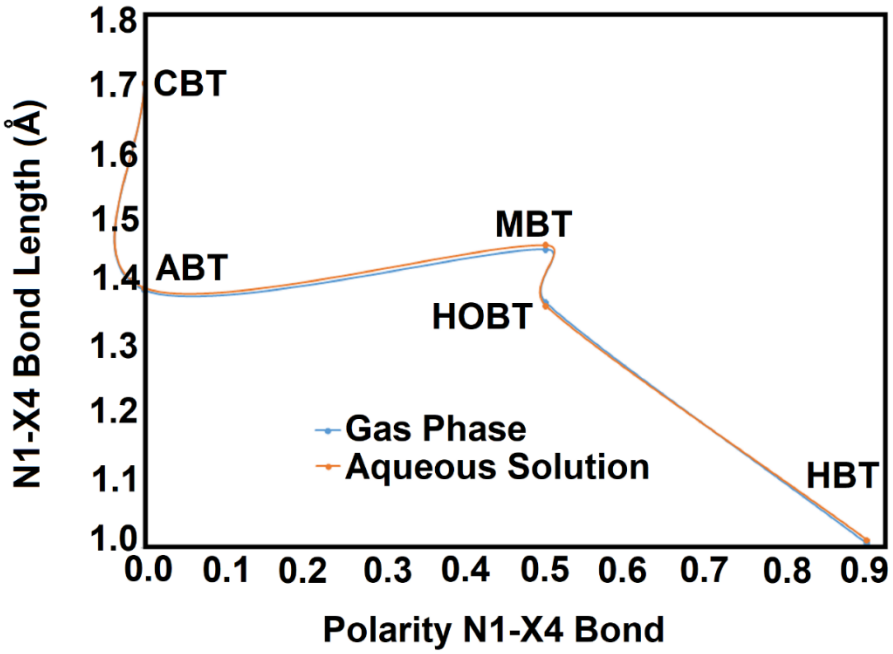

Figure S3. Variations of N1-X4 Bond Lengths of All of Members of the Series of 1-X-Benzotriazole Derivatives with X= H, CH_3, C_l, NH_2, and OH in Gas Phase and Aqueous Solution as Function of Polarity N1-X4 Bond by Using the B3LYP/6-311++G(d,p) Method

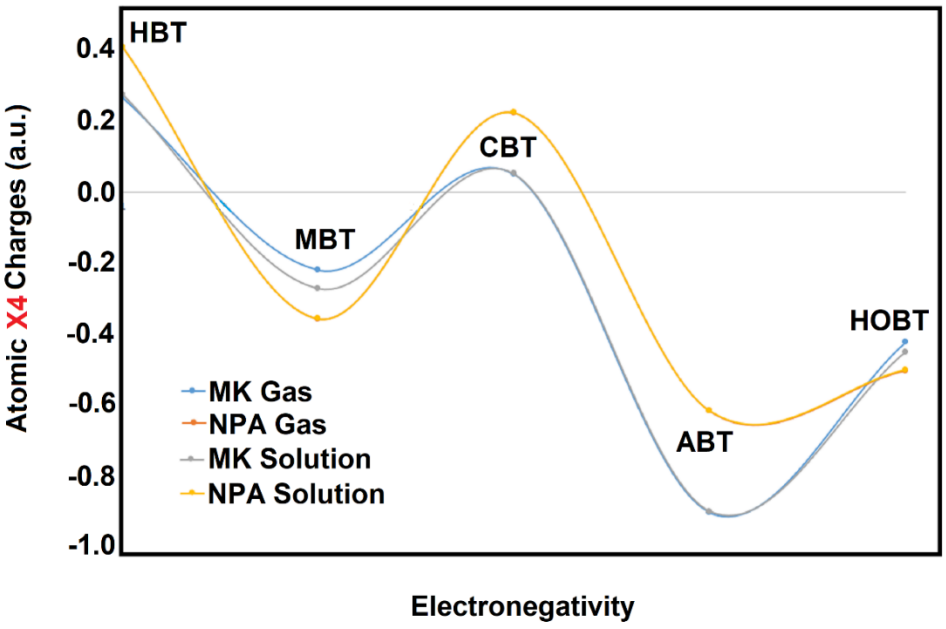

Figure S4. Variations of MK and NPA Charges on X4 Atoms of All of Members of the Series of 1-X-Benzotriazole Derivatives with X= H, CH_3, C_l, NH_2, and OH in Gas Phase and Aqueous Solution as Function of Electronegativity Groups by Using the B3LYP/6-311++G(d,p) Method

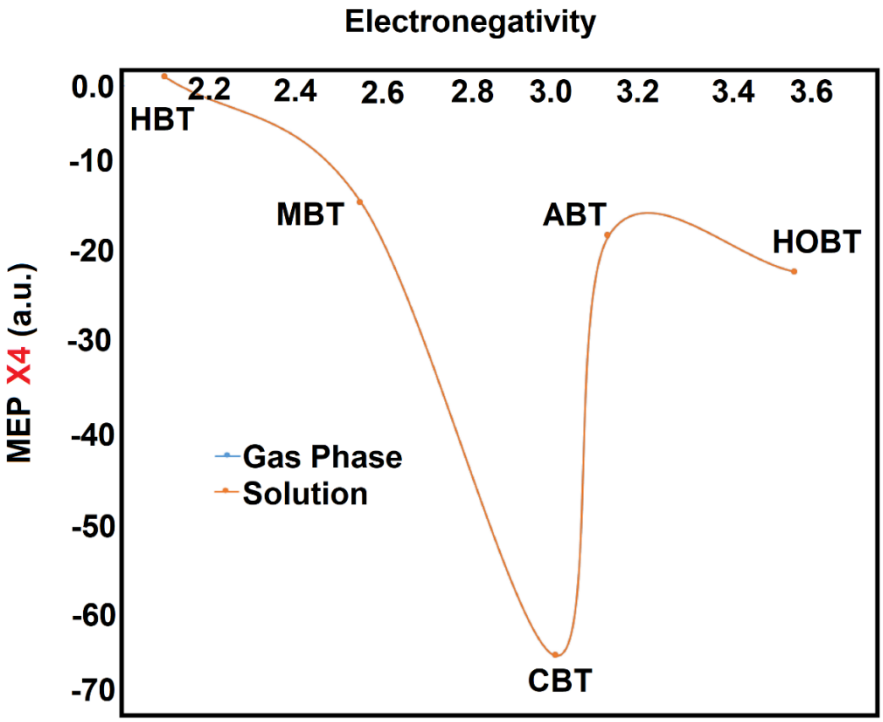

Figure S5. Variations of Molecular Electrostatic Potential (MEP) on X4 Atoms of All of Members of the Series of 1-X-Benzotriazole Derivatives with X= H, CH_3, C_l, NH_2, and OH in Gas Phase and Aqueous Solution as Function of Electronegativity Groups by Using the B3LYP/6-311++G(d,p) Method

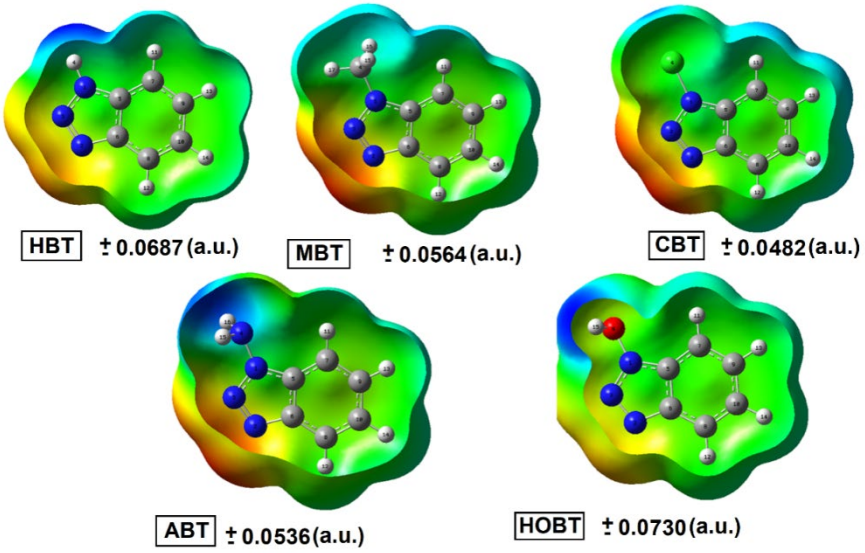

Figure S6. Calculated Electrostatic Potential Surfaces on the Molecular Surfaces of all Members of Series of 1-X-Benzotriazole Derivatives with X= H, CH_3, C_l, NH_2, and OH in Gas Phase by Using the B3LYP/6-311++G(d,p) Method. Isodensity Value of 0.005

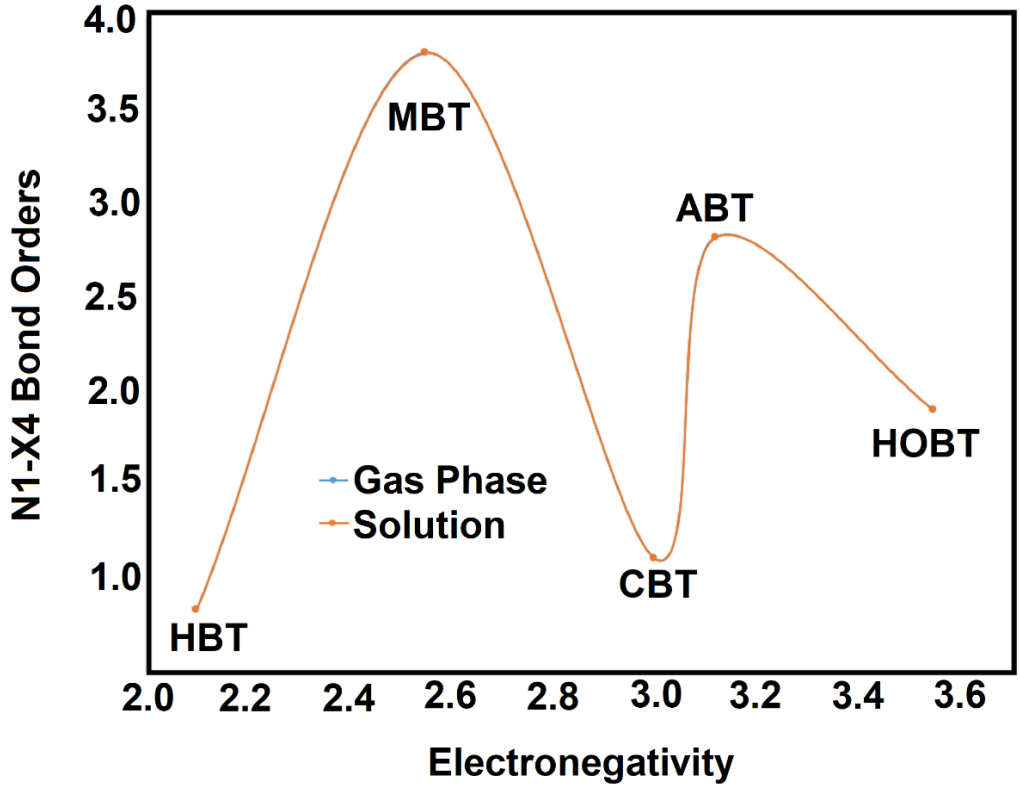

Figure S7. Variations of N1-X4 Bond Orders of All of Members of the Series of 1-X-Benzotriazole Derivatives with X= H, CH_3, C_l, NH_2, and OH in Gas Phase and Aqueous Solution as Function of Electronegativity Groups by Using the B3LYP/6-311++G(d,p) Method

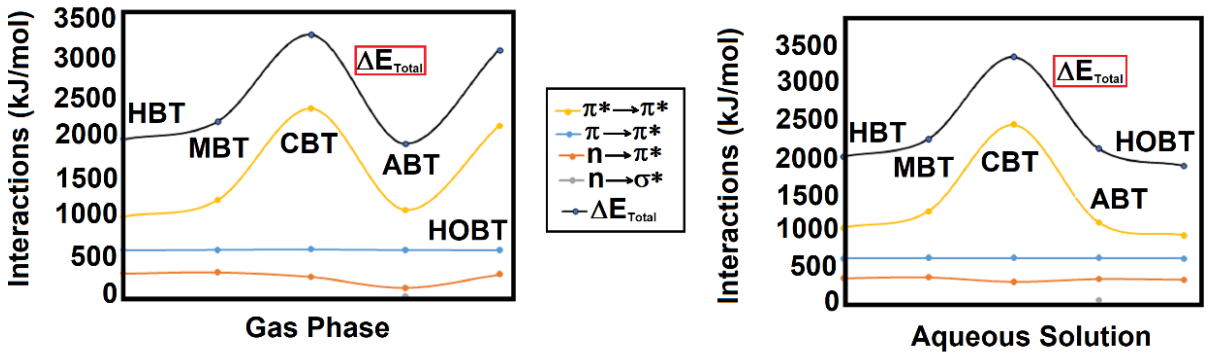

Figure S8. Main stabibilization energies of All of Members of the Series of 1-X-Benzotriazole Derivatives with X= H, CH_3, C_l, NH_2, and OH in Gas Phase and Aqueous Solution as Function of Electronegativity Groups by Using the B3LYP/6-311++G(d,p) Method

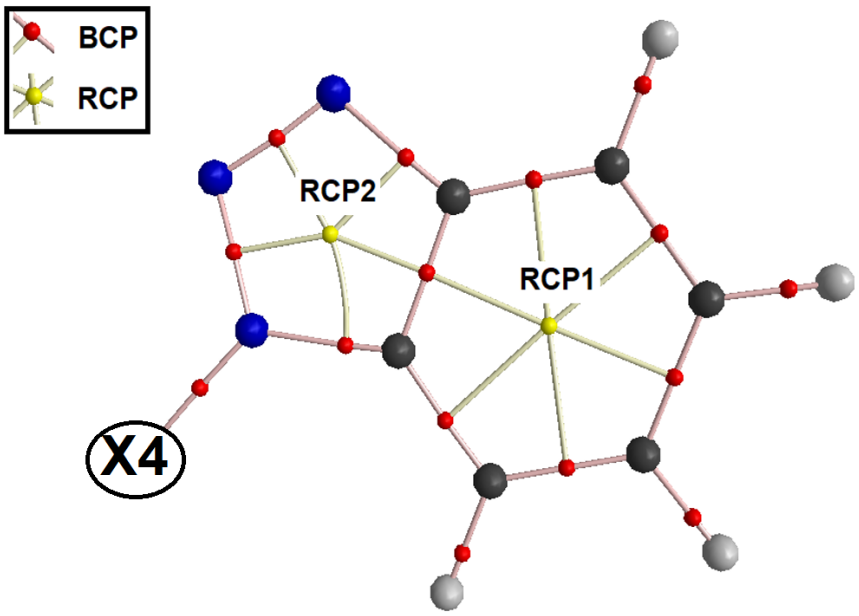

Figure S9. Details of the Molecular Models for All of Members of the Series of 1-X-Benzotriazole Derivatives with X= H, CH_3, Cl, NH_2, and OH in Gas Phase and Aqueous Solution as Function of Electronegativity Groups by Using the B3LYP/6-311++G(d,p) Method Showing the Geometries of All Their Ring Critical Points (RCPs)

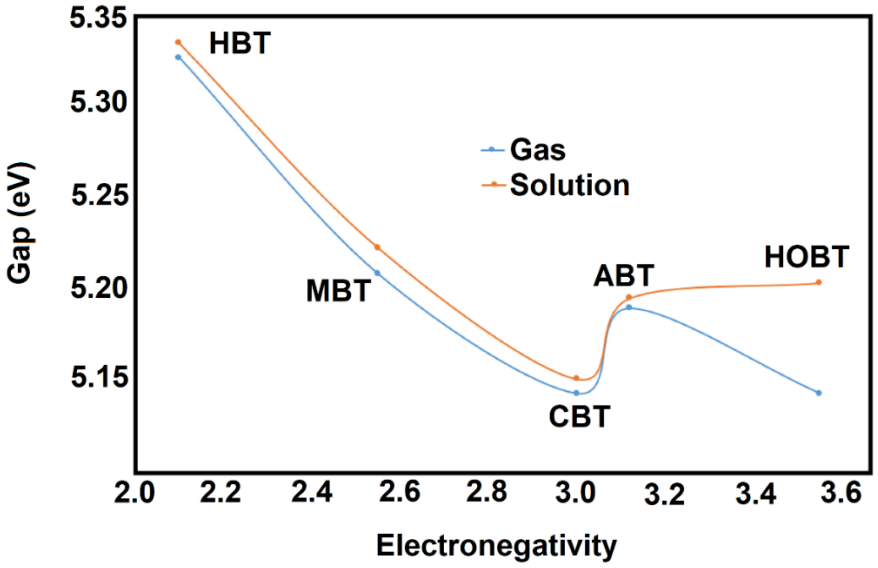

Figure S10. Variations of Gap Values of All of Members of the Series of 1-X-Benzotriazole Derivatives with X= H, CH_3, Cl, NH_2, and OH in Gas Phase and Aqueous Solution as Function of Electronegativity Groups by Using the B3LYP/6-311++G(d,p) Method

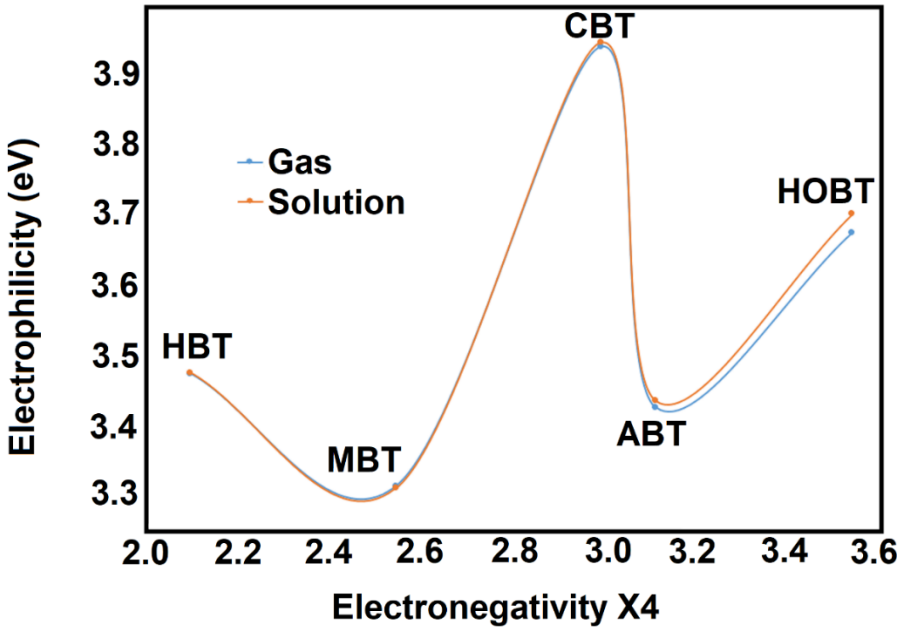

Figure S11. Variations of Global Electrophilicity Index (ω) of All of Members of the Series of 1-X-Benzotriazole Derivatives with X= H, CH_3, C_l, NH_2, and OH in Gas Phase and Aqueous Solution as Function of Electronegativity Groups by Using the B3LYP/6-311++G(d,p) Method

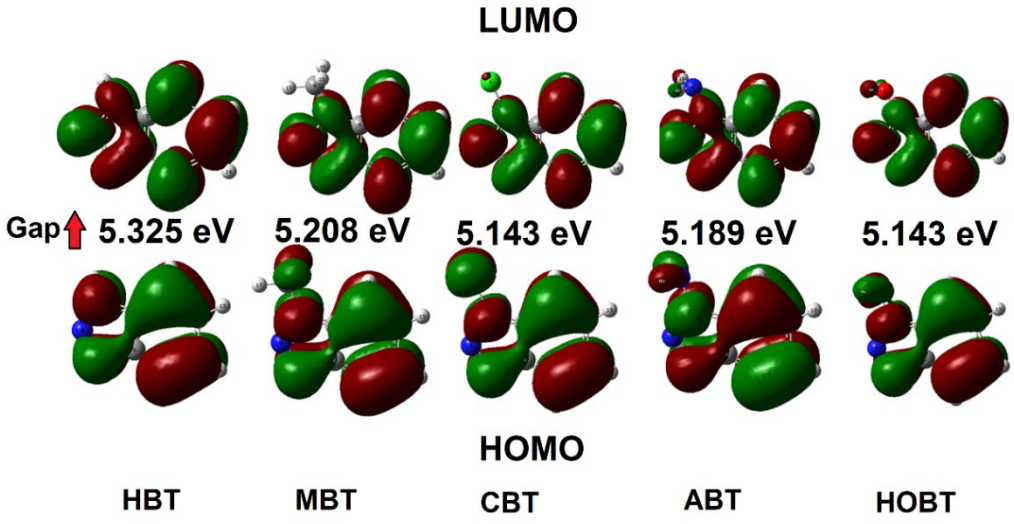

Figure S12. Comparisons Between the Frontier Orbitals HOMO-LUMO of All of Members of the Series of 1-X-Benzotriazole Derivatives with X= H, CH_3, C_l, NH_2, and the Gap Valuesin Gas Phaseby Using the B3LYP/6-311++G(d,p) Method

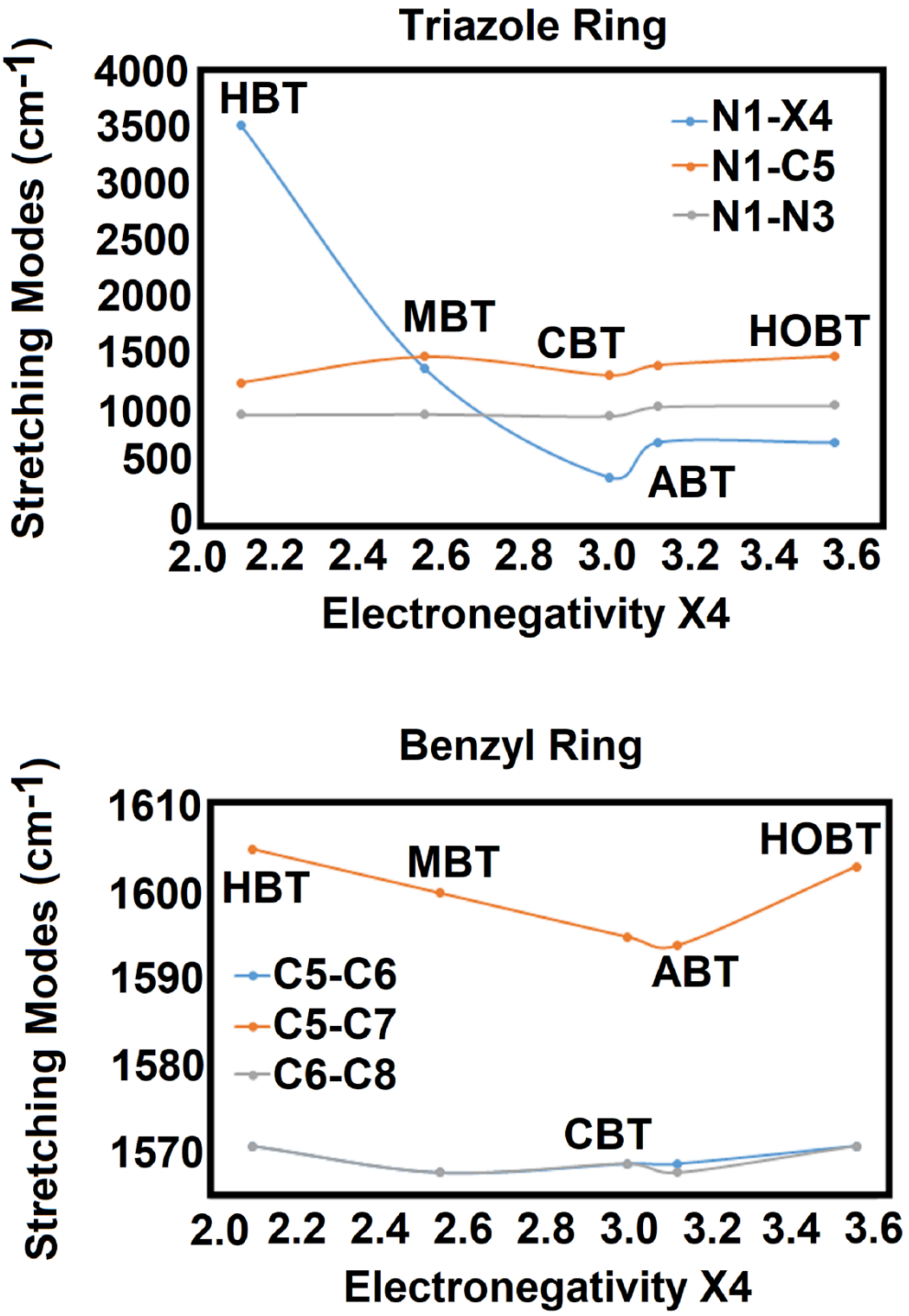

Figure S13. Correlations of Stretching N1-X4, N-N, C-C Modes of All of Members of the Series of 1-X-Benzotriazole Derivatives with X= H, CH_3, C_l, NH_2, and OH in Gas Phase and Aqueous Solution as Function of Electronegativity Groups by Using the B3LYP/6-311++G(d,p) Method

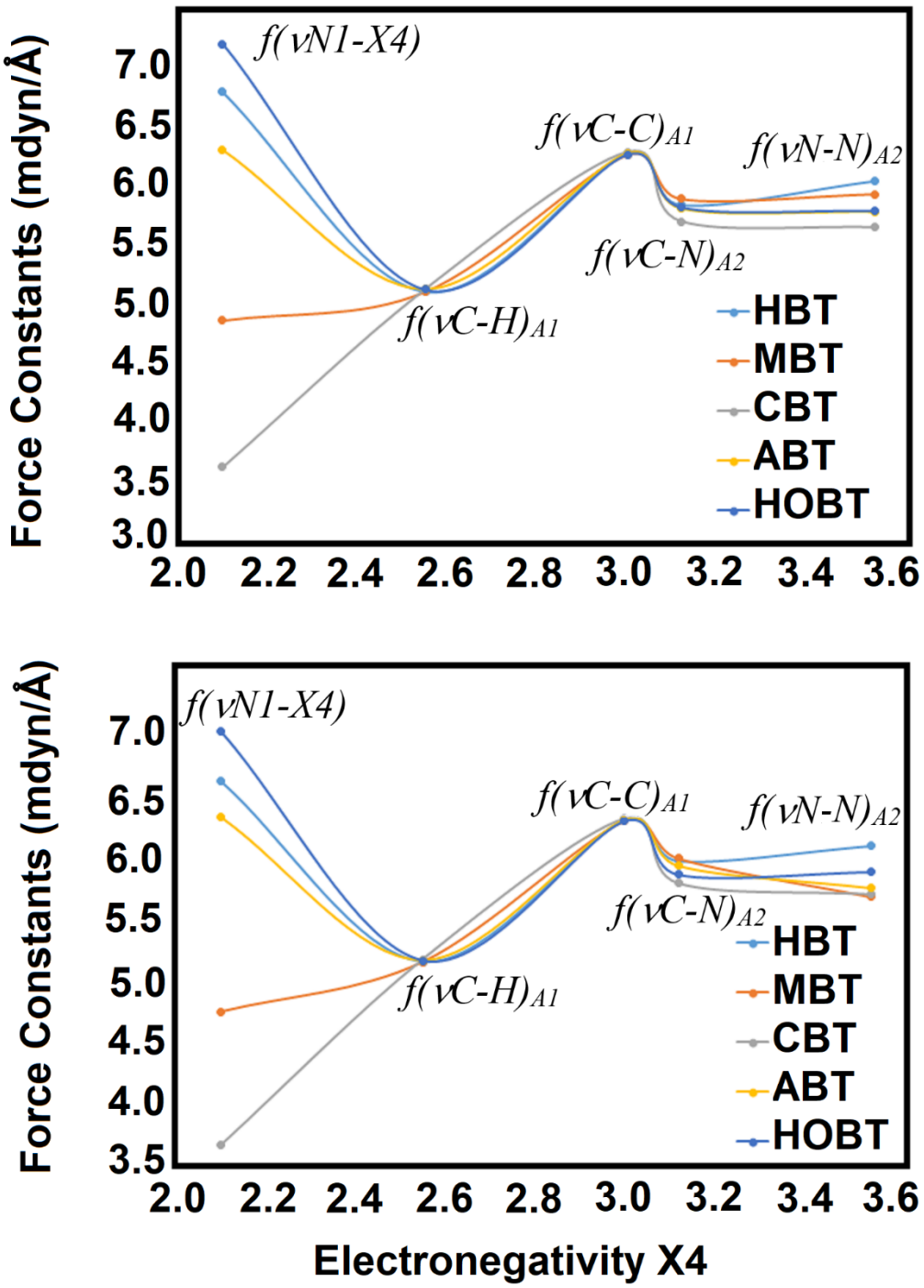

Figure S14. Variations of Scaled N1-X4, C-C, C-N and N-N, Force Constants of All of Members of the Series of 1-X-Benzotriazole Derivatives with X= H, CH_3, C_l, NH_2, and OH in Gas Phase and Aqueous Solution as Function of Electronegativity Groups by Using the B3LYP/6-311++G(d,p) Method

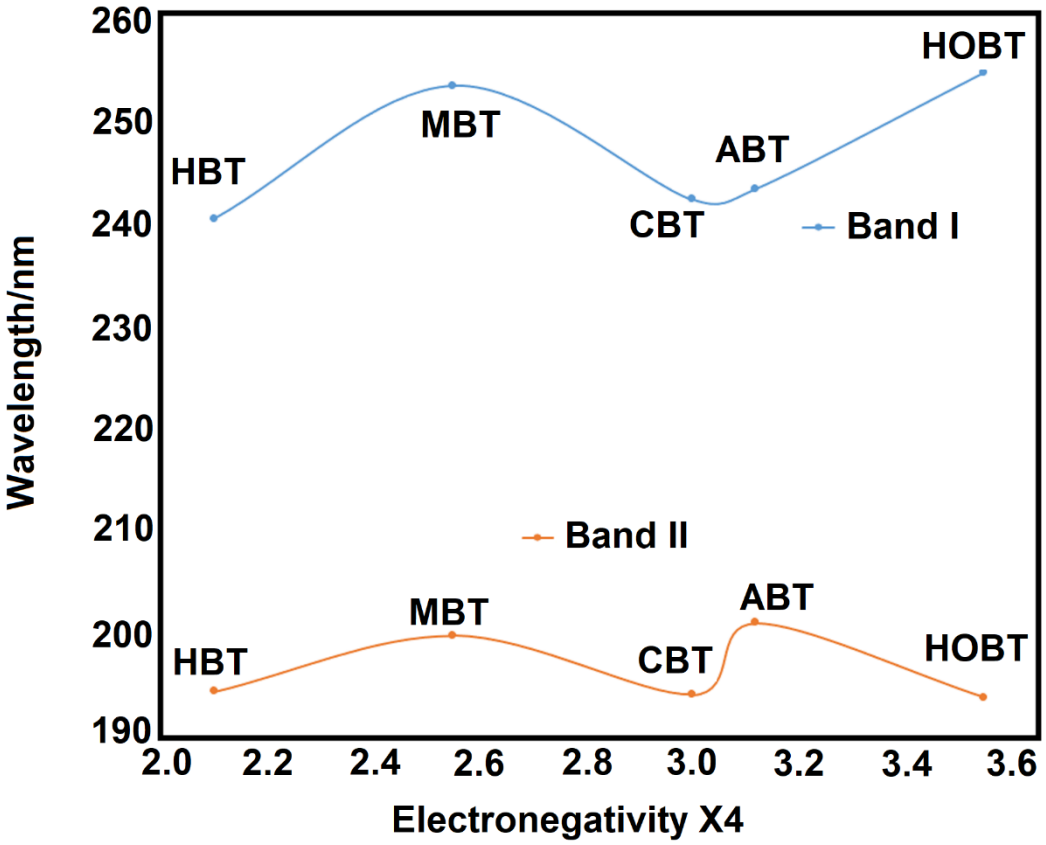

Figure S15. Variations in Positions of Two Bands of All of Members of the Series of 1-X-Benzotriazole Derivatives with X= H, CH_3, C_l, NH_2, and OH in Gas Phase and Aqueous Solution as Function of Electronegativity Groups by Using the B3LYP/6-311++G(d,p) Method

Appendix 2

Table 7. Observed and Calculated Wavenumbers (cm^{-1}) and Assignments for All Members of Series of 1-X-Benzotriazole Derivatives (X= H, CH_3, Cl, NH_2, OH) in Gas Phase by Using the B3LYP/6-311++G(d,p) Method

B3LYP/6-311++G** Method[a]									
HBT		MBT		CBT		ABT		HOBT	
SQM[b]	Assignments[a]	SQM[b]	Assignments[a]	SQM[b]	Assignments[a]	SQM[b]	Assignments[a]	SQM[b]	Assignments[a]
3507	νN1-H4					3413	$\nu_a NH_2$	3590	νO4-H15
						3338	$\nu_a NH_2$		
3070	νC8-H12	3069	νC8-H12	3072	νC7-H11	3073	νC7-H11	3074	νC7-H11
3061	νC7-H11	3061	νC7-H11	3069	νC8-H12	3068	νC8-H12	3069	νC8-H12
3052	νC10-H14	3051	νC10-H14	3056	νC10-H14	3053	νC10-H14	3055	νC10-H14
3040	νC9-H13	3039	νC9-H13	3044	νC9-H13	3040	νC9-H13	3043	νC9-H13
		3019	$\nu_a CH_3$						
		2966	$\nu_a CH_3$						
		2910	$\nu_s CH_3$						
						1623	δNH_2		
1605	νC5-C7	1600	νC5-C7	1595	νC5-C7	1594	νC5-C7	1603	νC5-C7
1571	νC5-C6,νC6-C8	1568	νC5-C6	1569	νC5-C6,νC6-C8	1568	νC5-C6,νC6-C8	1571	νC5-C6,νC6-C8
1483	βC10-H14,νC7-	1477	νC8-C10,νN1-	1472	βC10-H14	1478	νC8-C10	1483	βC10-H14,νC8-
1441	βC7-H11	1448	$\delta_{as} CH_3$						
		1435	$\delta_{as} CH_3$,βC8-	1426	βC7-H11	1433	βC8-H12,βC7-	1428	βC8-H12,βC7-H11
		1422	$\delta_{as} CH_3$					1416	δO4-H15,βC9-H13
		1398	$\delta_s CH_3$			1403	νN1-C5		
1378	βN1-H4	1372	$\delta_s CH_3$,νN1-C4	1363	νC7-C9	1364	νC9-C10,νC5-C6	1361	νC7-C9
1362	νC9-C10,βC9-	1361	νC9-C10,βC9-	1311	νN1-C5	1301	ϱNH_2	1289	βC8-H12,βC7-H11

1293	νN2-N3	1297	νN2-N3	1291	νN2-N3	1295	νN2-N3	1284	νN2-N3
1251	νN2-C6,βC8-	1286	βC7-H11	1260	βR_1(A2),νN1-C5	1284	βC7-H11	1272	δO4-H15
1247	νN1-C5	1230	νN2-C6	1221	νN2-C6	1225	νN2-C6	1226	νN2-C6
1207	νN2-C6	1190	ϱCH_3						
1135	βC9-H13	1149	βC9-H13,νC7-	1140	βC9-H13	1152	βC9-H13,νC7-	1147	βC9-H13,βC7-H11
1109	βC8-H12,νC8-	1114	ϱ'CH_3	1111	βC8-H12,νC8-	1121	βC8-H12,βC10-	1121	βC8-H12
1003	βR_1(A2)	1113	βC8-H12,βC10-	1041	βR_1(A2)	1099	βR_1(A1),βC7-	1092	βR_1(A1),νN1-O4
		1100	βR_1(A1),νC5-			1039	νN1-N3	1052	νN1-N3
981	νC9-C10	987	νC9-C10	985	νC9-C10	984	γC9-H13,γC10-	983	γC10-H14,γC9-H13
977	γC10-H14,γC9-	978	γC10-H14	982	γC10-H14,γC9-	983	νC9-C10	982	νC9-C10
969	νN1-N3	975	νN1-	958	νN1-N3				
942	γC8-H12	941	γC8-H12,γC9-	945	γC8-H12	950	γC8-H12	948	γC8-H12
902	βR_1(A1)	905	βR_1(A1)	908	βR_1(A1)	929	βR_1(A1),βR_2(A2)	917	βR_1(A1),βR_2(A2)
843	γC7-H11	844	γC7-H11	843	γC7-H11	852	γC7-H11	848	γC7-H11
						834	wagNH_2		
770	βR_3(A1),νC6-	775	νC6-C8	773	νC6-C8,νC5-C7	771	wagNH_2,βR_3(A1)	780	νC6-C8,βR_2(A1)
747	γC9-H13,γC7-	746	γC9-H13,γC7-	746	γC9-H13,γC7-	756	γC9-	750	γC9-H13,γC7-H11
728	τR_1(A1)	732	τR_1(A1),τR_1(A2)	723	τR_1(A1),τR_1(A2)	740	τR_1(A1),τR_1(A2)	734	τR_1(A1),τR_1(A2)
671	τR_2(A2)	721	νN1-C4	656	βR_2(A2)	724	νN1-N4	722	νN1-O4,βR_3(A1)
630	βR_2(A2)	643	τR_2(A2)	619	τR_2(A2),τR_1(A1)	637	τR_2(A2)	625	τR_2(A2)
		589	βR_1(A2)			594	βR_1(A2)	593	βR_1(A2)
562	τR_2(A1),τR_1(A1)	557	τR_2(A1),τR_2(A2)	557	βR_3(A1)	550	τR_2(A2),τR_2(A1)	542	τR_2(A2),τR_2(A1)
537	βR_3(A1)	527	βR_3(A1)	531	τR_2(A2)	530	βR_3(A1)	534	τR_2(A2),βR_3(A1)
450	γN1-H4	482	βR_2(A1)	472	βR_2(A1)	495	βR_2(A1)	500	βR_2(A1)
413	τR_3(A1),τR_2(A1)	416	τR_3(A1),τR_2(A1)	417	νN1-Cl4	424	τR_3(A1),τR_2(A1)		
407	βR_2(A1)			413	τR_3(A1),τR_2(A1)			415	τR_3(A1),τR_2(A1)
		275	γN1-C4,τR_2(A1)			272	γN1-N4,τR_2(A2)	266	γN1-O4,τR_2(A2)
252	τR_3(A1),τR_2(A2)	240	βN1-C4	245	τR_2(A2),γN1-Cl4	260	βN1-N4	257	γN1-O4,βN1-O4
197	ButC6-C5	211	ButC6-C5	202	ButC6-C5	223	ButC6-C5	208	ButC6-C5

		130	γN1-C4	183	βN1-Cl4	204	τwNH$_2$	190	τO4-H15
		87	τ$_w$CH$_3$	95	γN1-Cl4	137	γN1-N4	136	γN1-O4

Abbreviations: ν, stretching; β, deformation in the plane; γ, deformation out of plane; wag, wagging; τ, torsion; ρ, rocking; τw, twisting; δ, deformation; a, antisymmetric; s, symmetric; A1, Benzyl ring; A2, Triazole ring; [a]This work, [b]From SQMFF/B3LYP/6-311++G** method. 1-H-benzotriazole (HBT), 1-Methyl-benzotriazole (MBT), 1-Cl-benzotriazole (CBT), 1-Amino-benzotriazole (ABT) and 1-Hidroxy-benzotriazole (HOBT)

Table 8. Scaled Internal Force Constants for All Members of series of 1-X-Benzotriazole Derivatives (X= H, CH$_3$, C$_l$, NH$_2$, OH) in Gas Phase and Aqueous Solution by Using the B3LYP/6-311++G(d,p) Method

B3LYP/6-311++G** method										
Force constant	HBT		MBT		CBT		ABT		HOBT	
	Gas	Water	Gas	Water	Gas	Water	Gas	Water	Gas	Water
f(νN1-X4)	6.80	6.59	4.88	4.74	3.65	3.67	6.31	6.30	7.20	6.99
f(νC-H)$_{A1}$	5.12	5.14	5.12	5.14	5.14	5.16	5.14	5.15	5.14	5.15
f(νC-C)$_{A1}$	6.28	6.28	6.27	6.27	6.29	6.29	6.28	6.28	6.27	6.27
f(νC-N)$_{A2}$	5.85	5.95	5.90	5.97	5.71	5.77	5.82	5.91	5.83	5.84
f(νN-N)$_{A2}$	6.05	6.07	5.94	5.66	5.66	5.68	5.79	5.73	5.80	5.86

Note: Units are mdyn Å^{-1} for stretching. 1-H-benzotriazole (HBT), 1-Methyl-benzotriazole (MBT), 1-Cl-benzotriazole (CBT), 1-Amino-benzotriazole (ABT) and 1-Hidroxy-benzotriazole (HOBT)

Table S3. Analysis of the Bond Critical Points (BCPs) and Ring Critical Point (RCPs) for ATPO in Gas Phase and in Ethanol Solution by Using B3LYP/6-311++G(d,p) Calculations

GAS PHASE										
	1-H		**1-CH_3**		**1-Cl**		**1-NH_2**		**1-OH**	
Parameter [#]	RCP1	RCP2	RCP1	RCP2	RCP1	RCP2	RCP1	RCP2	RCP1	RCP2
$\rho(r)$	0.0213	0.0542	0.0214	0.0544	0.0215	0.0545	0.0214	0.0543	0.0214	0.0549
$\nabla^2\rho(r)$	0.1565	0.4426	0.1561	0.4388	0.1572	0.4314	0.1569	0.4332	0.1568	0.4353
AQUEOUS SOLUTION										
Parameter [#]	RCP1	RCP2	RCP1	RCP2	RCP1	RCP2	RCP1	RCP2	RCP1	RCP2
$\rho(r)$	0.0213	0.0546	0.0214	0.0547	0.0215	0.0547	0.0214	0.0546	0.0214	0.0551
$\nabla^2\rho(r)$	0.1563	0.4448	0.1560	0.4399	0.1572	0.4325	0.1566	0.4344	0.1568	0.4356

[#] Parameters in a.u.

Table S4. Frontier Molecular Orbitals, HOMO and LUMO, Gap Values and Chemical Potential (μ), Electronegativity (χ), Global Hardness (η), Global Softness (S) and Global Electrophilicity Index (ω) Descriptors for Monomer and Dimers of ABT in Gas Phase and Water Solution by Using B3LYP/6-311++G(d,p) Calculations

Orbital	**1-H**		**1-CH_3**		**1-Cl**		**1-NH_2**		**1-OH**	
	Gas	Water	Gas	Water	Gas	Water	Gas	Water	Gas	Water
HOMO	-6.966	-6.974	-6.762	-6.773	-7.072	-7.083	-6.8137	-6.8247	-6.920	-6.991
LUMO	-1.641	-1.641	-1.554	-1.551	-1.929	-1.932	-1.6245	-1.6300	-1.777	-1.788
|GAP|	5.325	5.333	5.208	5.222	5.143	5.151	5.1892	5.1947	5.143	5.203
DESCRIPTORS (eV)										
χ	4.3035	4.3075	4.1580	4.1620	4.5005	4.5075	4.2191	4.2273	4.3485	4.3895

Table S1. Merz-Kollman and NPA Charges (a.u.), Molecular Electrostatic Potentials (MEP) (a.u.) and Bond Orders, Expressed as Wiberg Indexes for the Series of 1X-Benzotriazole Derivatives (X= H, CH_3, Cl, NH_2, OH) in Gas Phase and Aqueous Solution by Using the B3LYP/6-311++G(d,p) Method

1H-BENZOTRIAZOLE (HBT)								
GAS PHASE					AQUEOUS SOLUTION			
Atoms	MK	NPA	MEP	BO	MK	NPA	MEP	BO
N1	-0.063	-0.361	-18.305	3.438	-0.085	-0.352	-18.302	3.447
N2	-0.415	-0.242	-18.376	3.110	-0.418	-0.247	-18.378	3.100
N3	-0.200	-0.037	-18.336	3.087	-0.198	-0.040	-18.337	3.086
X4	0.268	0.410	-0.968	0.835	0.276	0.410	-0.965	0.836
1-METHYLBENZOTRIAZOLE (MBT)								
N1	0.281	-0.228	-18.305	3.575	0.290	-0.220	-18.303	3.583
N2	-0.424	-0.247	-18.383	3.106	-0.434	-0.253	-18.384	3.096
N3	-0.229	-0.037	-18.344	3.083	-0.239	-0.039	-18.344	3.083
X4	-0.219	-0.357	-14.713	3.808	-0.271	-0.356	-14.711	3.807
1-CLBENZOTRIAZOLE (CBT)								
N1	0.012	-0.256	-18.257	3.517	0.010	-0.249	-18.256	3.524
N2	-0.392	-0.225	-18.363	3.135	-0.397	-0.229	-18.364	3.127
N3	-0.140	-0.023	-18.324	3.082	-0.140	-0.026	-18.325	3.082
X4	0.051	0.224	-64.330	1.110	0.053	0.225	-64.330	1.109
1-AMINOBENZOTRIAZOLE (ABT)								
N1	0.512	-0.081	-18.278	3.610	0.523	-0.075	-18.276	3.617
N2	-0.328	-0.241	-18.377	3.106	-0.336	-0.245	-18.378	3.098
N3	-0.339	-0.054	-18.340	3.082	-0.345	-0.057	-18.341	3.081
X4	-0.903	-0.617	-18.337	2.824	-0.900	-0.617	-18.336	2.821
1-HIDROXYBENZOTRIAZOLE (HOBT)								
N1	0.337	0.065	-18.247	3.617	0.423	0.069	-18.245	3.621
N2	-0.403	-0.245	-18.371	3.102	-0.394	-0.250	-18.372	3.095
N3	-0.223	-0.048	-18.331	3.084	-0.249	-0.038	-18.332	3.088
X4	-0.423	-0.503	-22.275	1.898	-0.451	-0.501	-22.274	1.898

Table S2. Main delocalization energies (in kJ/mol) for the Series of 1X-Benzotriazole Derivatives (X= H, CH_3, Cl, NH_2, OH) in Gas Phase and Aqueous Solution by Using the B3LYP/6-311++G(d,p) Method

Delocalization [a]	1-H	
	Gas	Water
$\pi N2\text{-}N3 \rightarrow \pi^*C5\text{-}C6$	58.39	60.74
$\pi C5\text{-}C6 \rightarrow \pi^*N2\text{-}N3$	111.65	114.53
$\pi C5\text{-}C6 \rightarrow \pi^*C7\text{-}C9$	67.84	67.67
$\pi C5\text{-}C6 \rightarrow \pi^*C8\text{-}C10$	74.11	72.02
$\pi C7\text{-}C9 \rightarrow \pi^*C5\text{-}C6$	82.60	81.18
$\pi C7\text{-}C9 \rightarrow \pi^*C8\text{-}C10$	67.80	67.38
$\pi C8\text{-}C10 \rightarrow \pi^*C5\text{-}C6$	72.73	72.31
$\pi C8\text{-}C10 \rightarrow \pi^*C7\text{-}C9$	84.65	82.68
$\Delta E_{\pi \rightarrow \pi^*}$	**619.77**	**618.51**

*LP(1)N1→π*N2-N3*	180.12	194.50
*LP(1)N1→π*C5-C6*	153.20	154.28
$\Delta E_{LP\rightarrow\pi^*}$	**333.31**	**348.78**
*π*N2-N3→π*C5-C6*	187.31	175.98
*π*C5-C6→π*C8-C10*	848.46	857.90
$\Delta E_{\pi^*\rightarrow\pi^*}$	**1035.76**	**1033.88**
ΔE_{TOTAL}	**1988.84**	**2001.18**
Delocalizationa	1-CH3	
	Gas	Water
*πN2-N3 →π*C5-C6*	60.11	62.57
*πC5-C6 →π*N2-N3*	114.66	115.45
*πC5-C6→π*C7-C9*	69.30	69.39
*πC5-C6→π*C8-C10*	74.53	72.40
*πC7-C9→π*C5-C6*	81.30	80.05
*πC7-C9→π*C8-C10*	67.63	67.34
*πC8-C10→π*C5-C6*	71.90	71.52
*πC8-C10→π*C7-C9*	84.19	82.30
$\Delta E_{\pi\rightarrow\pi^*}$	**623.61**	**621.02**
*LP(1)N1→π*C5-C6*	161.60	160.60
*LP(1)N1→π*N2-N3*	187.26	202.23
$\Delta E_{LP\rightarrow\pi^*}$	**348.86**	**362.82**
*π*N2-N3→π*C5-C6*	188.06	176.98
*π*C5-C6→π*C8-C10*	1047.17	1078.40
$\Delta E_{\pi^*\rightarrow\pi^*}$	**1235.23**	**1255.38**
ΔE_{TOTAL}	**2207.71**	**2239.23**
Delocalizationa	1-Cl	
	Gas	Water
*πN2-N3 →π*C5-C6*	58.73	60.61
*πC5-C6 →π*N2-N3*	115.83	116.91
*πC5-C6→π*C7-C9*	66.63	66.59
*πC5-C6→π*C8-C10*	72.48	70.89
*πC7-C9→π*C5-C6*	86.15	85.36
*πC7-C9→π*C8-C10*	68.55	68.26
*πC8-C10→π*C5-C6*	73.32	73.23
*πC8-C10→π*C7-C9*	84.27	83.01
$\Delta E_{\pi\rightarrow\pi^*}$	**625.96**	**624.87**
*LP(1)N1→π*C5-C6*	132.63	131.80
*LP(1)N1→π*N2-N3*	156.92	164.57
$\Delta E_{LP\rightarrow\pi^*}$	**289.55**	**296.36**
*π*N2-N3→π*C5-C6*	446.47	460.93
*π*C5-C6→π*C7-C9*	736.01	757.29
*π*C5-C6→π*C8-C10*	1182.48	1218.22
$\Delta E_{\pi^*\rightarrow\pi^*}$	**2364.96**	**2436.44**
ΔE_{TOTAL}	**3280.46**	**3357.67**
Delocalization [a]	1-NH_2	
	Gas	Water
*πN2-N3 →π*C5-C6*	57.31	59.27

*πC5-C6 →π*N2-N3*	117.54	119.55
*πC5-C6→ π*C7-C9*	66.63	66.59
*πC5-C6→ π*C8-C10*	73.94	72.23
*πC7-C9→ π*C5-C6*	84.27	82.81
*πC7-C9→ π*C8-C10*	69.01	68.97
*πC8-C10→ π*C5-C6*	71.10	71.19
*πC8-C10→ π*C7-C9*	82.18	80.80
$\Delta E_{\pi\rightarrow\pi^*}$	**621.98**	**621.40**
*LP(1)N1→ π*C5-C6*	150.02	150.06
*LP(1)N1→ π*N2-N3*	0.00	188.64
$\Delta E_{LP\rightarrow\pi^*}$	**150.02**	**338.71**
*LP(1)N4→σ*N1-N3*	46.36	45.19
$\Delta E_{LP\rightarrow\sigma^*}$	**46.36**	**45.19**
*π*N2-N3→ π*C5-C6*	171.05	164.69
*π*C5-C6→ π*C8-C10*	943.47	940.96
$\Delta E_{\pi^*\rightarrow\pi^*}$	**1114.51**	**1105.65**
ΔE_{TOTAL}	**1932.87**	**2110.95**
Delocalization [a]	1-OH	
	Gas	Water
*πN2-N3 →π*C5-C6*	60.11	62.20
*πC5-C6 →π*N2-N3*	115.41	114.16
*πC5-C6→ π*C7-C9*	66.96	67.59
*πC5-C6→ π*C8-C10*	71.69	70.35
*πC7-C9→ π*C5-C6*	83.47	82.85
*πC7-C9→ π*C8-C10*	68.26	67.76
*πC8-C10→ π*C5-C6*	72.23	72.40
*πC8-C10→ π*C7-C9*	82.89	82.22
$\Delta E_{\pi\rightarrow\pi^*}$	**621.02**	**619.52**
*LP(1)N1→ π*C5-C6*	139.90	141.37
*LP(1)N1→ π*N2-N3*	178.15	186.80
$\Delta E_{LP\rightarrow\pi^*}$	**318.06**	**328.17**
*π*N2-N3→ π*C5-C6*	182.08	176.48
*π*C5-C6→ π*C7-C9*	1237.91	0.00
*π*C5-C6→ π*C8-C10*	736.14	753.78
$\Delta E_{\pi^*\rightarrow\pi^*}$	**2156.13**	**930.26**
ΔE_{TOTAL}	**3095.21**	**1877.95**